REPUBLIC OF TURKEY
YILDIZ TECHNICAL UNIVERSITY
GRADUATE SCHOOL OF SCIENCE AND ENGINEERING

USING MICROFLUIDIC SYSTEMS FOR MICROALGAL BIOPROCESS AND BIOTECHNOLOGY

Beyza KARACAOĞLU

MASTER OF SCIENCE THESIS
Department of Bioengineering
Program of Bioengineering

Supervisor
Prof. Dr. Didem BALKANLI

Co-supervisor
Prof. Dr. Musa TÜRKER

January, 2024

REPUBLIC OF TURKEY
YILDIZ TECHNICAL UNIVERSITY
GRADUATE SCHOOL OF SCIENCE AND ENGINEERING

USING MICROFLUIDIC SYSTEMS FOR MICROALGAL BIOPROCESS AND BIOTECHNOLOGY

A thesis submitted by Beyza KARACAOĞLU in partial fulfillment of the requirements for the degree of **MASTER OF SCIENCE** is approved by the committee on 02.01.2024 in Department of Bioengineering, Program of Bioengineering.

Prof. Dr. Didem BALKANLI
Yildiz Technical University
Supervisor

Prof. Dr. Musa TÜRKER
Yildiz Technical University
Co-supervisor

Approved By the Examining Committee

Prof. Dr. Didem BALKANLI, Supervisor
Yildiz Technical University _____

Assoc. Prof. Dr. Tuğba ÖZER, Member
Yildiz Technical University _____

Prof. Dr. Ali KOŞAR, Member
Sabanci University _____

I hereby declare that I have obtained the required legal permissions during data collection and exploitation procedures, that I have made the in-text citations and cited the references properly, that I haven't falsified and/or fabricated research data and results of the study and that I have abided by the principles of the scientific research and ethics during my Thesis Study under the title of Using Microfluidic Systems for Microalgal Bioprocess and Biotechnology supervised by my supervisor, Prof. Dr. Didem BALKANLI. In the case of a discovery of false statement, I am to acknowledge any legal consequence.

Beyza KARACAOĞLU

Signature

This work was supported by the the project no “123M415 of The Scientific and Technological Research Council of Turkey Tubitak, 2210-A Domestic General Master’s Scholarship Program and under the auspices of the Presidency of the Republic of Turkey, the Ministry of Industry and Technology of the Republic of Turkey and the coordination of TÜBİTAK MAM Polar Research Institute”

Dedicated to my family
my dog
and my besties
For their endless love and support

ACKNOWLEDGEMENTS

I express my gratitude to my advisor, Professor Dr. Didem Balkanlı, for her unwavering academic and psychological support throughout my academic journey and for coordinating the laboratory where I performed all of my research endeavors, as well as to my co-advisor, Professor Dr. Musa Türker. I would like to thank Assist. Prof. Dr. Benan İnan and Dr. Anıl Tevfik Koçer for generously imparting their expertise to me, guiding my path in academia, and providing invaluable support and assistance. I would like to express my appreciation to my teammates at the Algal Biotechnology and Bioprocess Laboratory, Res. Assist. Gülcan Ayşin Karaca, PhD Student Hilal Kabakçı, MSc Student Elif Göksu Kızılyar, and BSc students Barkın Balcı, Demir Oleksiy Karasu, Dilek Bozkurt and Ozan Aydın for their invaluable support.

I would also like to thank Prof. Dr. Ali Koşar for coordinating the laboratory where I performed microfluidic research for my thesis, and thank PhD student İsmail Bütün and MSc student Rabia Mercimek for generously sharing their extensive expertise on microfluidic systems and providing valuable assistance in both the practical and theoretical aspects.

This study was supported under the auspices of the Presidency of the Republic of Turkey, the Ministry of Industry and Technology of the Republic of Turkey, and the coordination of the TÜBİTAK MAM Polar Research Institute, by TÜBİTAK 1002-123M415 project and by 2210-A Domestic General Master's Scholarship Program.

Ultimately, I wish to express my gratitude to my family and friends for their encouragement and support during this journey. Thank you to my mother, father, and brother, İlban Karacaoğlu, Mehmet Refik Karacaoğlu, and Demir Karacaoğlu, my beloved dog Weasley, and my dear friends Ece Ayhan, Ceren Sert, Selcan Akar, Maria Orlenco and Hilal Çalık.

Beyza KARACAOĞLU

TABLE OF CONTENTS

LIST OF SYMBOLS viii

LIST OF ABBREVIATIONS ix

LIST OF FIGURES x

LIST OF TABLES xii

ABSTRACT xiii

ÖZET xv

1 INTRODUCTION 1

1.1 Literature Review 1

1.2 Objective of the Thesis 2

1.3 Original Contribution 3

2 GENERAL INFORMATION 5

2.1 Microalgae 5

2.1.1 Polar Microalgae 7

2.2 Microfluidic System Technology 10

2.3 Microfluidics for Microalgal Bioprocess and Biotechnology 12

2.3.1 Microalgae Cultivation 12

2.3.2 Microalgal Separation Process 14

2.3.3 Microfluidic Devices as Algal Biosensor 21

3 MATERIALS AND METHODS 23

3.1 Determination of Microorganism Sizes in Samples from Antarctica and Microorganism Selection 23

3.2 Microorganism Cultivation 24

3.2.1 Selecting Microorganisms to Assess Separation Performance 24

3.2.2 Microalgae Cultivation 25

3.2.3 Bacteria Cultivation 26

3.3 Design and Microfabrication of Microfluidic Platforms 27

3.4 Experimental Set-up with Microfluidics as A Novel Technology . . 34
3.4.1 Preliminary Preparation 34
3.4.2 Separation Process Experiments Using Microfluidic Method 35
3.4.3 Determination of Separation Performance of Microfluidic Platforms 36
3.4.4 Re-cultivation of Microalgae After Separation Using a Selected Microfluidic Platform 36
3.5 Experimental Set-up with Antibiotics as A Traditional Method . . . 37
3.6 Determination of Biochemical Contents After Microalgae Cultivation 38
3.6.1 Phenol-Sulfuric Acid Method for Carbohydrate Determination 38
3.6.2 Protein Analysis (Modified Lowry Method) 38
3.6.3 Spectrophotometric pigment analysis 38

4 CONCLUSION **40**
4.1 Result and Discussion 40
4.1.1 Microorganism Sizes in Antarctic Samples 40
4.1.2 Microalgae Growth Kinetics 42
4.1.3 Design and Microfabrication of Microfluidic Platforms . . . 42
4.1.4 Separation Performance of Microfluidic Platforms 47
4.1.5 Separation Performance of Antibiotic-Treatment Method . . 54
4.1.6 Comparing Biochemical Contents and Growth Kinetics of Microalgae Cultures After Novel and Traditional Separation Methods 55
4.2 Conclusion and Future Perspectives 57

REFERENCES **60**

A APPENDIX CHAPTER HEADING **72**
A.1 Microfabricated PDMS-based Microfluidic Platforms 72

PUBLICATIONS FROM THE THESIS **73**

LIST OF SYMBOLS

U_f	Average fluid velocity
$^{\circ}C$	Centigrade
F_D	Drag Force
U_{De}	Dean velocity
ρf	Fluid density
μ	Fluid viscosity
D_h	Hydraulic diameter of microchannel
αp	Microparticle diameter
N_{A_final}	Number of microalgae at final
N_{A_0}	Number of microalgae at inlet
N_{A_i}	Number of microalgae at outlet i
N_{onset}	Number of total microorganism at beginning
N_{final}	Number of total microorganism at final
N_{Total_0}	Number of total microorganism at inlet
N_{Total}	Number of total microorganism at outlets
N_{Total_i}	Number of total microorganism at outlet i
π	Pi
R	Radius of curvature

LIST OF ABBREVIATIONS

2D	Two dimensional
CO_2	Carbon dioxide
cm	Centimeter
De	Dean Number
DEP	Dielectrophoresis
DW	Distilled water
FDA	Food and Drug Administration
LCA	Life Cycle Analysis
IPA	Isopropyl alcohol
μ m	Micrometer
μ g	Microgram
μ L	Microliter
mL	Milliliter
min	Minute
NB	Nutrient Broth
NA	Nutrient Agar
PFF	Pinched Flow Fractionation
PDMS	Polydimethylsiloxane
Re	Reynolds Number
TAE-III	Third National Antarctic Science Expedition
UV	Ultraviolet light

LIST OF FIGURES

Figure 2.1 Adaptation mechanisms of polar microalgae [3] 8
Figure 2.2 Benefits, applications, and drawbacks of microfluidic systems . 10
Figure 2.3 Standard soft lithography method (A. Mold fabrication steps; B.PDMS based fabrication) [67, 68] 11
Figure 2.4 Microfluidic device for lipid production from microalgae (A) Schematic presentation of micro-droplet based system. (B) Layout of device for light intensity effect. [6, 82] 13
Figure 2.5 Adsorption and loading phase for microalgae cultivation in microchambers. [6, 86] 14
Figure 2.6 Microfluidic separation techniques 15
Figure 2.7 Active separation methods in microfluidics [6] 16
Figure 2.8 Lateral DEP-based microfluidic device to detect the microalgae with highest lipid content [6, 102] 17
Figure 2.9 Passive separation methods in microfluidics [6] 18
Figure 2.10 Astaxanthin accumulation in microfluidic platform [6, 128] . . . 21
Figure 2.11 High-throughput screening for microalgal strains in microfluidic platform [6] 22
Figure 3.1 Kerman Brand Incubator, Wiseshake orbital shaker 25
Figure 3.2 *C. minutissima* cultures 26
Figure 3.3 *E. coli* after 24-hours incubation 27
Figure 3.4 Silicon wafer coating process with PR-Su-8 3050 photoresist . . 31
Figure 3.5 Development process 32
Figure 3.6 Vacuuming of PDMS 32
Figure 3.7 Silicon wafer coated by PDMS 33
Figure 3.8 PDMS microchannels after oxygen plasma bonding 33
Figure 3.9 A cross-sectional image of PDMS microchannels under a light microscope 34
Figure 3.10 Microfluidic experimental set-up 35
Figure 4.1 Antarctic samples after gram staining under a light microscope at a magnification of 100X 41
Figure 4.2 Cell size distribution for Antarctic microorganisms 41
Figure 4.3 Growth kinetics of *Chlorella minutissima* 42

Figure 4.4 *Chlorella minutissima* cultivation in photobioreactor 43
Figure 4.5 *Chlorella minutissima* at logarithmic phase 43
Figure 4.6 Microfluidic platform designs 46
Figure 4.7 Separation of microalgae from bacteria in spiral microchannels . 47
Figure 4.8 Relationship between separation yield as a function of Reynolds number 49
Figure 4.9 Relationship between separation purity and Reynolds number . 50
Figure 4.10 Relationship between enrichment factor and Reynolds number . 51
Figure 4.11 Growth kinetics of three different microalgae culture 57
Figure A.1 PDMS-based microfluidic platforms 72

LIST OF TABLES

Table 3.1 Gram staining steps 24
Table 3.2 Design parameters of microfluidic platforms for microalgae separation 28
Table 3.3 Materials for microfabrication steps 29
Table 3.4 Equipment for microfabrication steps 30
Table 3.5 Reagents prepared for protein analysis 39
Table 4.1 Velocities of different flow rates in microfluidics 44
Table 4.2 Reynolds number and Dean number calculations 44
Table 4.3 Dean velocity and drag forces calculations 45
Table 4.4 Separation performance of microfluidic platforms 48
Table 4.5 Separation performance of antibiotic-treatment method in microalgae cultures 54
Table 4.6 Comparing biochemical contents of microalgae cultures 56

ABSTRACT

Using Microfluidic Systems for Microalgal Bioprocess and Biotechnology

Beyza KARACAOĞLU

Department of Bioengineering
Master of Science Thesis

Supervisor: Prof. Dr. Didem BALKANLI
Co-supervisor: Prof. Dr. Musa TÜRKER

Polar microalgae are quite astonishing species because of their rich metabolic diversity and protection mechanisms to survive under various harsh conditions. In this context, it is important to detect and evaluate polar microalgae with higher bioactive contents. The downstream process of microalgae production is essential for the development and their use in various industries but also has critical importance in biomass, productivity, and product quality. Microfluidic technologies aim to overcome the drawbacks of conventional methods, achieve efficient separation of microalgae, minimize energy consumption, costs, and chemicals, and standardize the experiment. A microfabricated microfluidic device, including spiral microchannels, was developed to separate microalgae and bacteria based on their sizes. The separation performance of the microfluidic system was examined, and the reculturability and biochemical composition of the separated microalgae were evaluated. A comparison was made between the microfluidic method and the antibiotic-mediated cultivation and serial dilution methods in terms of growth and biochemical analysis results. According to the results, the separation process led to a high efficiency of up to 90%, a purity of up to 95%, and a post-chip enrichment factor of up to 1.2. Also, microalgae cultures with antibiotic disks exhibited a decline in both microalgae growth and biochemical content. In contrast, the utilization of advanced microfluidic technology demonstrated that microalgae exhibited significant levels of longevity as well as a higher growth rate and biochemical contents in comparison to pure microalgae culture. Furthermore,

this research has demonstrated that the optimized microfluidic platform has the potential for isolating microalgae from Antarctica, eliminating contaminants, and enhancing the growth and composition of microalgae for microalgal biotechnology.

Keywords: Microalgae, microfluidic systems, separation process, Antarctica, biotechnology.

ÖZET

Mikroakışkan Sistemlerin Mikroalgal Biyoproses ve Biyoteknolojide Kullanımı

Beyza KARACAOĞLU

Biyomühendislik Anabilim Dalı
Yüksek Lisans Tezi

Danışman: Prof. Dr. Didem BALKANLI
Eş-Danışman: Prof. Dr. Musa TÜRKER

Kutup mikroalgleri, zengin metabolik çeşitlilikleri ve çeşitli zorlu koşullar altında hayatta kalabilmelerini sağlayan koruma mekanizmaları nedeniyle oldukça şaşırtıcı türlerdir. Bu bağlamda biyoaktif içerikleri daha yüksek olan kutup mikroalglerinin tespiti ve değerlendirilmesi önemlidir. Mikroalg üretiminin alt prosesi, bunların çeşitli endüstrilerde geliştirilmesi ve kullanılması için esastır ancak aynı zamanda biyokütle, ürün verimliliği ve kalitesi üzerinde de kritik öneme sahiptir. Mikroakışkan teknolojileri, geleneksel yöntemlerin dezavantajlarını ortadan kaldırmak, mikroalgleri yüksek verimlilikle ayırmak, enerji, kimyasal madde ve inokulümü azaltmak, laboratuvarda harcanan zamanı önemli ölçüde azaltmak ve deneyi standartlaştırmak için seçilmiştir. Ön aşamada 3. Ulusal Antarktika Bilim Seferi'nden getirilen ve karakterizasyonu tamamlanmış kutup örneklerinden farklı mikroorganizmaların türlerine ve boyutlarına göre ayrıştırılması işlemi için spiral mikrokanallara sahip yeni bir mikroakışkan cihaz tasarlanmıştır. Yumuşak litografi yöntemi ile mikroçip üretimi ve seçilen mikroorganizmalar ile optimizasyon çalışmalarının ardından, atalet mikroakışkanlarında hidrodinamik kuvvetler kullanılarak mikroalgler karışık Antarktika örneklerinden %90'a varan ayırma verimliliği, %95'e varan ayırma saflığı ve çip sonrası 1,2'ye varan zenginleştirme faktörü ile ayrıştırılmıştır. Mikroakışkan sistemin ayırma performansı belirlendikten sonra ayrılan mikroalglerin yeniden kültürlenebilirliği ve biyokimyasal içerikleri belirlenmiştir. Mikroakışkan yöntem ve elde edilen büyüme ve biyokimyasal analiz sonuçları antibiyotik ile kültivasyon ve seri

seyreltme yöntemleriyle karşılaştırılmıştır. Antibiyotik disk ile kültive edilen mikroalg kültürlerinde, mikroalg büyümesi ve biyokimyasal içeriklerinde saf kültüre göre azalış olduğu görülmüştür. Aksine, mikroakışkan platformun kullanımıyla mikroalglerin yüksek düzeyde canlılık gösterdiği, büyüme hızının ve biyokimyasal içeriklerin saf kültüre göre arttığı görülmüştür. Bu araştırma ile optimize edilen mikroakışkan platformun ayırma ve izolasyon proseslerinde kullanım potansiyelinin yanı sıra kültürün kontaminantlardan elimine edilmesinde ve mikroalglerin artan büyüme ve içerikleri ile yöntemin mikroalgal biyoteknolojide kullanım potansiyelinin olduğu da kanıtlanmıştır.

Anahtar Kelimeler: Mikroalg, mikroakışkan sistemler, ayırma işlemleri, Antarktika, biyoteknoloji.

1
INTRODUCTION

1.1 Literature Review

Algae, primary producers in various environments, are essential for ecosystems. Microalgae, single-celled organisms, are crucial due to their high-value biomass, sustainable raw materials, and carbon dioxide (CO_2) absorption capabilities. They have antiviral, anticancer, and antifungal effects and can integrate carbon into compounds. Microalgae can grow in a variety of environments, including the sea, soil, ocean, lake, and even polar regions, and they represent an essential component of the ecosystem [1, 2].

The polar regions are home to a wide range of microorganisms, including viruses, prokaryotes, bacteria, fungi, amoeba, archaea, and algae. Algae flourish during the melting phase because of increased water, nutrients, and radiation. Polar microalgae have a higher concentration of ATP synthase protein in their chloroplasts, as well as an increased presence of unsaturated fatty acids and antioxidants in their structures, in comparison to temperate microalgae. Furthermore, they possess adaptations to low-light conditions, an enhanced ability to absorb light, and ice-binding proteins incorporated into their structure [3].

The development of microfluidic system technologies encompasses various scientific disciplines, including physics, fluid mechanics, mechatronics, chemistry, and biology. These technologies often entail the use of micro-sized channels to generate microscale heat and fluid flow. This emerging methodology is employed across various bioengineering domains owing to its numerous benefits, including enhanced efficacy when working with small amounts of fluids, heightened sensitivity, efficient process regulation, diminished chemical and sample requirements, and a decreased number of experiments and reactor residence time [4]. These devices are especially prominent in fields such as microreactors, microbioreactors, separation processes, organ-on-a-chips, the development of diagnostic kits for viruses, and drug formulation [5]. Microfluidics is mostly

utilized in microalgal bioprocess and biotechnology for cultivation, separation and purification, and biosensor applications [6, 7]. Polydimethylsiloxane (PDMS), known for its transparency and gas permeability, is commonly employed in the manufacture of microfluidic platforms. This material offers flexibility in microchannel design and enables the passage of various flows. As a result, microalgae can be cultured under light for extended periods [8, 9]. Thanks to the adaptable microchannel geometries, variations in size between microorganisms, and the ability to have multiple inlet and outlet channels, microfluidics can also be employed in the subsequent stages of microalgae processing. This includes pre-treatments like harvesting, separation, extraction, and mechanical compression [6, 10, 11]. Due to the presence of chlorophyll pigments and the variations in capacitance across cells, these organisms can be effectively utilized in biosensor applications and microfluidics research for detecting microalgae in wastewater [12, 13].

1.2 Objective of the Thesis

The main objective of the thesis is the development of a new microfluidic platform for the separation and enrichment of microalgae from polar samples containing mixed microbial communities and to observe the effect of microfluidic treatment on microalgal growth and their biochemical contents. A model system was established to separate and characterize microalgae for isolation from Antarctica, with a preference for applying microfluidic techniques for this objective.

Samples collected from the environment, such as the sea, lake, glacier, desert, and volcano, contain a variety of microorganisms; therefore, the need to obtain a pure culture from a mixed microbial community using several methods for separation and purification has emerged.

Apart from microalgae isolation, microfluidic platforms can be used to obtain pure microalgae culture and to remove impurities from contaminated cultures. Obtaining a pure microalgae culture is crucial for various scientific, industrial, and environmental applications.

Nevertheless, the number of experiments necessary for optimization in traditional separation and purification processes is enormous, as are the volumes of inoculum, nutrient medium, and chemicals utilized. In this case, scientists investigated other strategies to avoid wasting time and energy. It is recommended within the scope of the thesis to develop a microfluidic bioprocess for the separation step to reduce time and energy consumption, as well as decrease the laboratory area,

parallelize experimental sets, and provide a more controlled separation process with *in situ* analysis and imaging. Furthermore, it is intended to avoid the installation of any external power in the microfluidic platform, which is designed to avoid operational complexity, to make the system simple and applicable, to minimize the energy consumed for the separation process, and to perform the separation process solely through the use of microchannel geometry. This passive approach separates microalgae from other microbial species in polar samples based on size. Because the sizes of bacteria, amoeba, and microalgae detected in polar samples brought back from Antarctica are numerous, it is presumed that the method based on hydrodynamic forces is appropriate for microalgae microfluidic separation. Microchannel geometry and channel parameters will be developed, manufactured, and optimized in this direction according to the sizes of microorganisms in Antarctic samples.

The objective of the system design is to use platforms consisting of spiral microfluidic microchannels with different design parameters and flow rates and to select the most suitable separation and microalgae enrichment process for Antarctic microalgae. Therefore, the optimization studies were carried out, and the impact of both flow parameters and channel geometry factors on separation performance was assessed.

The purpose of combining microfluidic technology with bioprocesses is to maximize separation performance. Since it is aimed to increase efficiency, microchannel geometry parameters and flow rate optimization studies will be carried out. Simultaneously with the separation process to be carried out using microfluidic technology, it is aimed to culture Antarctic samples, treat them with antibiotics, and set serial dilutions. This will allow for the quantitative and qualitative comparison of the microfluidic platform's benefits and drawbacks with the conventional approach. It is intended to re-cultivate samples before and after microfluidic separation processes in order to control and sustain the viability of Antarctic microalgae. The thesis aims to investigate and compare the biochemical contents of polar microalgae cultures, both purified using conventional methods and microfluidic technology.

1.3 Original Contribution

A spiral microfluidic platform will be presented in the literature to be used in various microalgal biotechnology fields once the potential and advantages of microfluidic systems in microalgal bioprocesses have been identified. This thesis evaluates the

following items, which have not been found in the literature before.

The research for the thesis contributes an original perspective to the literature on:

- Microfabrication of spiral microchannels for separating microalgae from Antarctica and increase their concentration.
- Comparison of separation method with antibiotic method in microfluidic systems in terms of biochemical content and growth kinetics of microalgae.
- To increase the separation performance, three different numbers of circles, two different distance between circles and five different flow rates were examined on microfabricated microfluidic platforms.
- To investigate the effect of distance between circles and the synergetic effects of distance between circles and the number of circles in microalgae separation.
- Analyzing the effect of number of circles and distance of them on the microalgal growth and biochemical content.
- Separating *Chlorella minutissima* microalgae from *Escherichia coli* bacteria.

Furthermore, there is not any investigation in Turkey integrating microfluidic systems and algal bioprocesses. The usage of microalgae in the microfluidic platform was carried out in one study [14], which was a Turkey-Germany partnership to design new-generation microrobots for medical drug delivery systems. Microalgae served in the study as living models because of their motility and phototaxis capabilities.

2
GENERAL INFORMATION

An increase in the global temperature of the world by 1.1°C was detected as a result of rising greenhouse gas concentrations brought on by an expanding human population throughout the centuries, as of 2022. Due to environmental changes brought on by global warming, the atmosphere and ocean circulations have altered, influencing the ecosystem. In addition to rising human populations, rising fossil fuel consumption and agricultural greenhouse gas concentrations significantly contribute to rising CO_2 levels. Climate change occurs through shifting seasons, shifting precipitation patterns, an increase in natural disasters, and rising sea levels caused by glacier melt [15–17]. Many researchers have reported that upon glacial melting, a single polar microalgae can proliferate and cover hundreds of square meters. Polar microalgae are becoming recognized as a key factor contributing to climate change. It is crucial to isolate and utilize bioactive-rich microalgae species that thrive in severe environments and emerge from melting glaciers in these polar regions for biotechnological purposes [18].

2.1 Microalgae

Algae are primary producers that can exist in a variety of environments, including the sea, soil, ocean, lake, glacier, and desert, and they represent an essential component of the ecosystem. Algae can be systematically classified into nine groups, with the main dividing factor being their pigment composition. The major groups include Rhodophyceae (red algae), Bacillariophyceae (diatoms), Pyrrophyceae (dinoflagellates), Phaeophyceae (brown algae), and Chlorophyceae (green algae). Because of their metabolic and enzymatic processes, they can use waste as a food source, they can be used in energy production as they produce biofuel precursors and fatty acids, and they can be consumed as healthy foods due to their high nutritional content [1, 19, 20].

Microalgae are a single-celled, eukaryotic organism crucial to the ecosystem

because they present high-value components from the biomass they produce. They are a sustainable source of raw materials, and can photosynthesize with light and absorb CO_2. Microalgae have biological capabilities such as antiviral, anticancer, antibacterial, and antifungal effects, and their ability to acquire and fix CO_2 allows them to integrate carbon into the structure of various compounds such as polysaccharides, proteins, lipids, vitamins, pigments, antioxidants, and inorganic salts [2, 21].

Microalgae have higher growth rates than plants and parameters such as temperature, pH, and nutrient medium, and their concentrations affect biomass production [22]. The biomass produced at the end of the process has the potential to be used in the preparation of high-value-added products including beta-carotene, astaxanthin, phycocyanin, superoxide dismutase, and omega-3 fatty acids, which are used in a variety of industries as food, bioplastics, cosmetics, healthcare, bioenergy, and wastewater treatment [23, 24]. For instance, FDA has approved phycocyanin, which is found in algae, for use as a natural food coloring. Similarly, astaxanthin's strong antioxidant levels have drawn interest from several industries [25].

Likewise, by promoting microalgal photosynthesis or artificial photosynthesis, these unique characteristics of microalgae might reduce the amount of CO_2 in the atmosphere and produce valuable components in a sustainable manner that contributes to both nature and the economy [26]. Microalgae allow them to have a minimal carbon footprint. An organelle within this process known as a pyrenoid raises the CO_2 content surrounding the thylakoid membranes. The photosynthetic enzyme ribulose-1,5-bisphosphate carboxylase/oxygenase (RUBISCO), which is responsible for absorbing carbon and has a low affinity for CO_2, becomes more active as the concentration of CO_2 increases [27]. However, since they are grown in the laboratory, particularly under artificial light, their bioprocesses need to be carefully designed in terms of lighting, light source selection, and energy consumption for the optimum ambient temperature because lightning and temperature are important parameters for microalgal cultivation. For instance, in a microalgae cultivation process, if the light intensity is insufficient, the respiration rate will be higher than photosynthesis, and microalgal biomass cannot be produced. On the contrary, if the light intensity is excessive, photo-oxidative damage occurs and leads to the death of microalgae. In order to ensure heat and mass transfer at maximum efficiency, proper bioreactor selection and configuration design are required. As of right now, life-cycle assessment (LCA), may serve as a useful technique for creating more sustainable and environmentally friendly designs which ensures that bioprocesses have a low carbon footprint. It is preferable to utilize

renewable energy sources or to provide heat and carbon from flue gas or waste heat [21, 26, 28].

2.1.1 Polar Microalgae

Along with the over 25 million-year history of algae, the formation of the Arctic and Antarctica has been estimated to have occurred 6 million and 25 million years ago, respectively [29]. Ocean levels are influenced by the seasonal creation and melting of glaciers, which is a result of global warming since glaciers comprise an important percentage of the ocean's surface area. Spring leads to it the highest sea ice level, which is reached in September in Antarctica and March in the Arctic [30]. It has been observed that when sea ice levels are compared between historical and current values, the Arctic sea ice cover has diminished and its surface area has reduced relative to the Antarctica [31]. On the other hand, significant drops in Antarctic sea ice covers have been noted since 2016. Although climate change is the cause of this scenario, atmospheric circulations and oceanographic conditions—that is, geographic location—have a greater influence on changes in the Arctic and Antarctica [31, 32]. Furthermore, micro-nutrient levels were shown to have a declining trends in the summer in the Arctic, whereas micro-nutrient levels remain constant throughout the year in the Antarctic location [33]. Aside from these alterations, the Arctic and Antarctica are distinguished by extremely cold temperatures, limited carbon resource availability, and irregular photo-periods [34].

In polar regions, microbial communities include viruses, prokaryotes, and eukaryotes, including bacteria, fungi, amoeba, algae, and archaea [35–37]. However, Antarctic region is often known for its major endemism, whereas the Arctic is home to only a handful of endemic species due to their different oceanic and geographical locations [33]. Even with its harsh environment, which includes low temperatures, high radiation and oxygen levels, high salinity, low phosphorus, and limited gas exchange, Antarctica is host to a wide variety of microalgae species [38].

Polar algae are extreme microorganisms that inhabit snow, soil, glaciers, lakes, oceans, and seas. In polar regions, liquid water, nutrients, and photosynthetically active radiation enhance during the melt period, and algal blooms also expand [39]. Algae play a key role in the phenomenon of global warming because they perform photosynthesis and absorb sunlight, which causes glaciers and snowy regions to melt more quickly. As melting progresses, algae growth accelerates [40]. Also, because of their disparate oceans and geographic environments, the microalgae

populations in the Arctic and Antarctic are highly unique [33].

Antarctica is inhabited to a rich range of metabolically diverse microorganisms that have not yet been cultivated or recognized, can survive in harsh, unexplored, and inaccessible environments, and have evolved various defense mechanisms to prevent cell damage and/or destruction [41]. Through genetic material recombination and horizontal exchange, this drives evolution. These organisms therefore serve as a resource for the identification of unknown species as well as unknown physiological mechanisms and genes of adaptability, as seen in Figure 2.1 which displays adaptation mechanisms of polar microalgae. Because its enormous potential for producing novel antibiotics, pigments, proteins, and other metabolites as well as beneficial biological activities, this region is extremely important. In this context, microorganisms that inhabit the poles draw interest from the biotechnology society and their potential applications in a variety of fields, including food, medicine, and materials science, make them an important topic for research and development [3, 42, 43]. In addition, recent research efforts demonstrated that polar microalgae species had the capacity to effectively degrade biodiesel at low temperatures using phytoremediation techniques, while also enhancing diesel hydrocarbons and promoting lipid synthesis [44, 45].

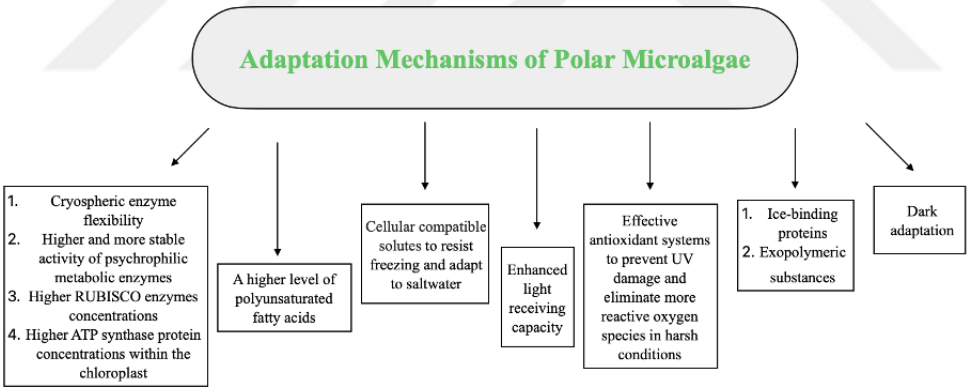


Figure 2.1 Adaptation mechanisms of polar microalgae [3]

Soto et al. [40] and Luo et al. [46] examined microbial communities in snow types of different colors taken from the Fildes Peninsula on King George Island. The color of the snow varies based on the type of algae present and the phase they are in; it may appear green when the algae produces primary metabolites and increases chlorophyll and red when the algae becomes stressed and produces astaxanthin [47]. The investigation by Luo et al. reported the identification of numerous species of green algae belonging to the *Chlorophyta* and *Ochrophyta* taxons. *Trebouxiophyceae*, *Ulvophyceae*, and *Chrysophyta* were predominant in green snow samples, but *Sanguina*, *Chloromonas*, *Trebouxiophyceae*, and *Chlainomonas* sp. were prevalent in red snow samples. *Proteobacteria* and *Bacteroidetes*

were found to be the most prevalent microbial communities in the samples, with the *Polaromonas* strain being the one with the greatest diversity. Furthermore, fungus and cercozoa were found in the samples. Remarkably, the study's findings revealed that the growth of snow algae depends on the presence of the *Polaromonas* genus of *Bacteroidetes*. Similarly, Soto et al. [40] found that Proteobacteria and Bacteroidetes were the most common bacterial groups, with the Trebouxiophyceae and Chlorophyceae green algae classes dominating over eukaryotes and a high abundance of the Stramenopile class. According to the outcomes, algae, which were reported to be the majority species, are dependent on photosynthetic parameters, and photosynthetic parameters are dependent on environmental parameters, light conditions, geographical locations, and snow colors [33].

The two most crucial challenges with polar microalgae lie in cultivating these species in the laboratory and tracking the effect of temperature on biomass and metabolite synthesis. Related research indicates that polar microalgae may be cultivated in laboratory environments and tolerate a range of temperatures; however, the extent of their tolerance and behaviour towards stress conditions varied throughout various species [48]. Numerous Arctic and Antarctic microalgae species appear to be psychrotolerant organisms rather than psychrophiles [49], despite the fact that other cold water algae are psychrophile organisms that cannot grow at temperatures over 20°C [50, 51]. Basically, it was found that while they may tolerate temperatures as low as 4°C, their growth accelerates at 20°C and higher, and they can even survive at 30°C [49, 52]. A number polar microalgae grow more effectively at 20°C than at lower temperatures. This is because the microalgae cannot get enough nitrate from the environment at lower temperatures. Instead, they increase the production of enzymes and, consequently, the amount of protein in order to maintain photosynthesis rates [49, 53]. For instance, Anuwar et. al. [54] underlined that the various strains of the same polar microalgae species may grow at different temperatures but their biochemical contents might change as well. In this study, two different polar *Chlorella* strains were grown at 4, 8 and 12°C. The results of the investigation showed that while the amount of pigment and carbohydrates increased with temperature, the amount of protein decreased. Similar findings were reported by Cao et al. [55] when they examined Arctic *Chlorella* in the temperature range of 3 and 27°C. They discovered that 15°C temperature was the optimum for specific growth and temperatures above 15°C enhanced the amount of protein and lipids as well as the synthesis of soluble sugar. The Antarctic *Chlorella* species' growth and metabolite synthesis were investigated by Inan et al. [49] as a function of temperature, nitrate, and light cycle. The results indicated that microalgae growth peaked at 27°C, in a 16:8 light-dark cycle, and at high nitrate concentrations.

In another study, the anticancer activity of Antarctic microalgae extracts and their potential for use in pharmaceutical applications were demonstrated. It was demonstrated that *P. endiviifolia* from Antarctic seaweeds was effective against lung and glioma cells [56], and *C. variabilis* and *C. pyrenoidosa* from Antarctic microalgae were efficient against prostatic and gastric adenocarcinoma cells [57].

2.2 Microfluidic System Technology

Microfluidic systems offer a highly effective tool in many disciplines such as bioengineering. Advancements in this field have triggered a profound impact on several fields, such as genetics, medicine, the pharmaceutical, food industry, and diagnostic kit systems [58]. Microfluidic technologies have contributed to the development of small fluidic systems, such as 3D microchannel structures with inner diameters ranging from 1 to 100 micrometers. Microfluidics is a discipline that specifically concentrates on the accurate regulation and handling of fluid dynamics and pressures at a size smaller than one millimeter. Furthermore, microfluidics facilitates the development of organ-on-a-chip systems that mimic certain organ characteristics and functions [59]. Figure 2.2 summarizes the applications, benefits, and drawbacks of microfluidic systems in the field of bioengineering [5, 60, 61].

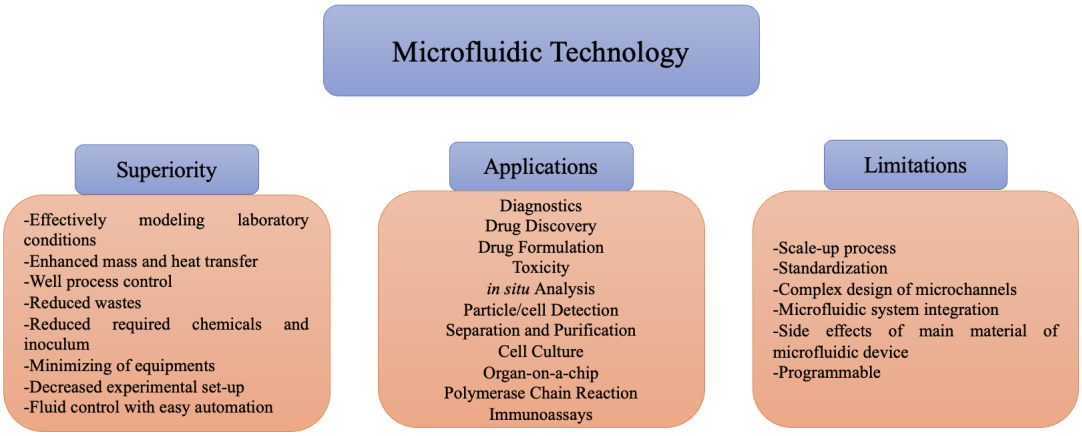


Figure 2.2 Benefits, applications, and drawbacks of microfluidic systems

Microfluidic systems primarily comprise input channels, output channels, and channel mixers. Furthermore, it may encompass components such as external power sources, valves, fittings, micropumps, and microseparators. Microfluidic system fabricate involves the utilization of materials such as silicon, glass, thermosets, thermoplastics, and paper [62, 63]. The fabrication process employs techniques like lithography, 3D printing, injection molding, and etching [64, 65]. In the field of microalgal bioprocess applications using microfluidic systems, the most prevalent

method is the conventional soft lithography technique with a PDMS-based approach [6, 7]. The variety of applications for microfluidic chips was extended with the advent of PDMS-based microfluidic devices. Because of their excellent optical transparency, flexibility, and biocompatibility, photolithographically manufactured masters can be used to efficiently imitate PDMS devices for a wide range of applications [5]. Figure 2.3 illustrates the procedural steps for standard soft lithography [66].

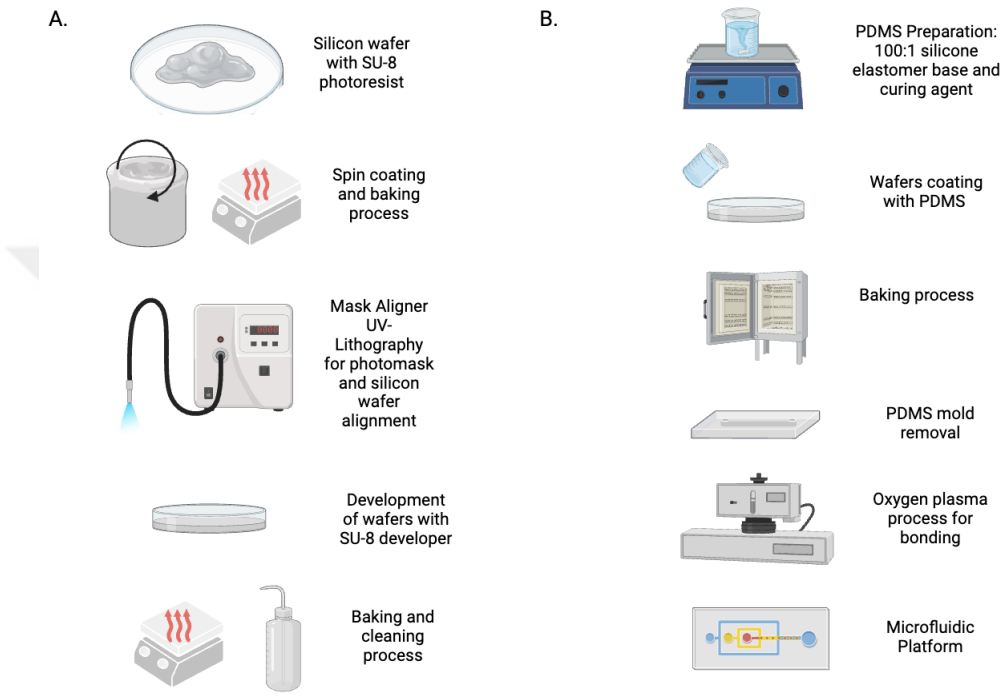


Figure 2.3 Standard soft lithography method (A. Mold fabrication steps; B.PDMS based fabrication) [67, 68]

Microfluidic devices, which often include T-junctions, flow-focusing, and co-flowing geometries, are routinely used to generate droplets with a uniform size distribution. Three-dimensional co-flowing microfluidic devices fully enclose the inner phase with the outer phase, thereby eliminating the impact of channel wall wettability on droplet formation. As a result, these devices are often used in the production of droplets. Within the wider context of microfluidic systems, the production of biomaterials usually depends on continuous and multiphase fluidic systems, which may be further classified as either droplet-based flows or co-flows [69]. Also, flow parameters such as flow rate and flow rate ratio should be considered and regulated from researchers because it is impacting several elements such as reaction kinetics, mixing efficiency, cell viability, and the overall functionality of microfluidic devices.

The geometry of microchannels in microfluidic device is an essential variable in

microfluidic systems due to its substantial impact on the system's functionality and efficacy in practical applications. Microchannels may be rectangular, spiral, serpentine, triangle, or linear, among other shapes. The microchannel geometry has a direct impact on the ratio of surface area to volume, as well as on the efficiency of heat and mass transport [70]. Additionally, it plays a crucial role in the classification and separation of particles or cells. The flow movement in microchannels is determined by the various structures of the channel geometries and their corresponding characteristics, such as channel width, channel height, and channel length. These factors influence the flow rate and flow rate ratios. Also, it is worth noting that the flow regime observed in microfluidic devices typically exhibits laminar flow. Hence, microchannel geometry can be employed as an alternative to external equipment in active methods for facilitating mixing, particularly in cell processes that are susceptible to collapse, such as microalgae, or in reactions that necessitate thorough mixing [71–73].

2.3 Microfluidics for Microalgal Bioprocess and Biotechnology

2.3.1 Microalgae Cultivation

Many researchers have recently focused on the cultivation of microalgae as a means of producing biomass, and studies are being conducted to attain concentrated microalgae production because of its usage in bioenergy and the accumulation of primary and secondary metabolites as highly valuable biological products in biomass [74, 75]. However, prior to bulk production, small-scale studies are critical to optimize these conditions for cultivation and to assess the growth profile of the microalgae strain by modeling its growth kinetics, as well as reducing cost, energy, and time consumption [76, 77]. It is appropriate to take advantage of microfluidic devices in such a scenario to maximize the synthesis of metabolites and biomass, appreciate the kinetics of microalgae biomass, to identify the metabolic processes of a single cell and to perform high-throughput screening for microalgae [78–80].

Microdroplet-based devices are frequently used for microalgae cultivation. These systems were chosen to observe the effect of light intensity and nutrient composition on the growth of *C. vulgaris* [81] and to increase the lipid production efficiency from *Botryococcus braunii* [82]. These systems, which are based on cell suspension and a carrier oil, contain thousands of cells in their droplets and provide a suitable environment for their cultivation. As an example Mishra et al. investigated the relationship between microalgae growth and lipid synthesis by adjusting numerous factors on the same chip utilizing the system they designed as demonstrated in Figure 2.4 [6, 82].

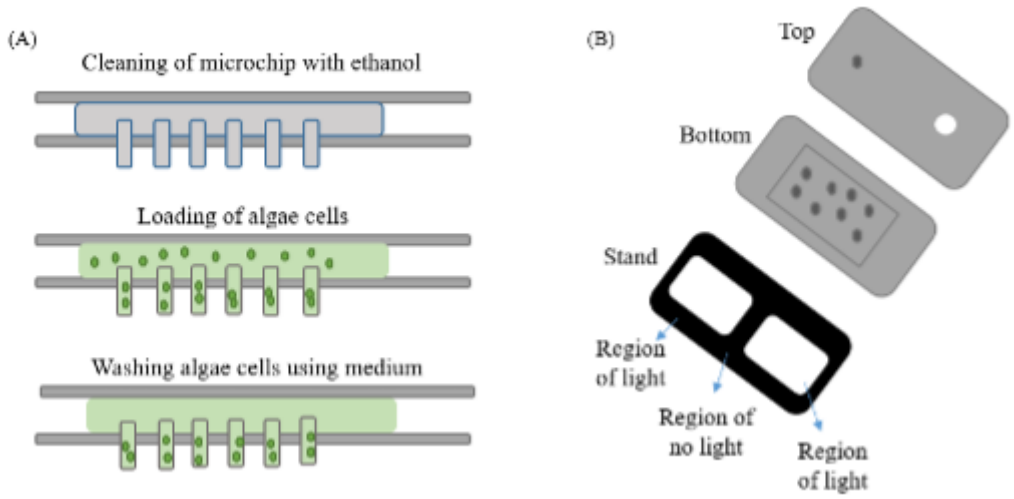


Figure 2.4 Microfluidic device for lipid production from microalgae (A) Schematic presentation of micro-droplet based system. (B) Layout of device for light intensity effect. [6, 82]

As another approach, microbioreactors/microphotobioreactors have garnered a lot of interest for small-scale cultivation approaches. Long-term microalgae cultivation may be possible with platforms having numerous micro-chambers which offer controlled conditions such as temperature, light, and nutrient [83].

Microbioreactors have been used to increase the synthesis of lipids from *B. braunii* by optimizing light intensity [79], to increase the production of secondary metabolites from *Chlamydomonas reinhardtii* by optimizing nutrient medium composition [8], and to increase the production of astaxanthin from *Haematococcus pluvialis* [9]. Paik et al. has two modules in their microfluidic platform design, and these modules allowed nutrient concentration arrangement and microalgae cultivation [8]. Microfluidic systems are also important in detecting the synergetic effects of different stress conditions on microalgae growth. Their module microsystems are more advantageous compared to traditional methods because they allow continuous feeding for microalgae [84, 85].

In a different design, a loading phase was constructed to independently inject the nutrient medium containing three different concentrations of sodium carbonate into the microphotobioreactor, and a CO_2 absorption phase was developed to obtain CO_2-rich liquid for the cultivation of *Scenedesmus obliquus* as illustrated in Figure 2.5 [86]. Also, Abdulla et al. fabricated a combined microfluidic differential carbonator with a microfluidic CO_2 gradient generator and a microculture chamber to production of *Picochlorum* sp. with different light intensities and CO_2 inlet concentrations [87].

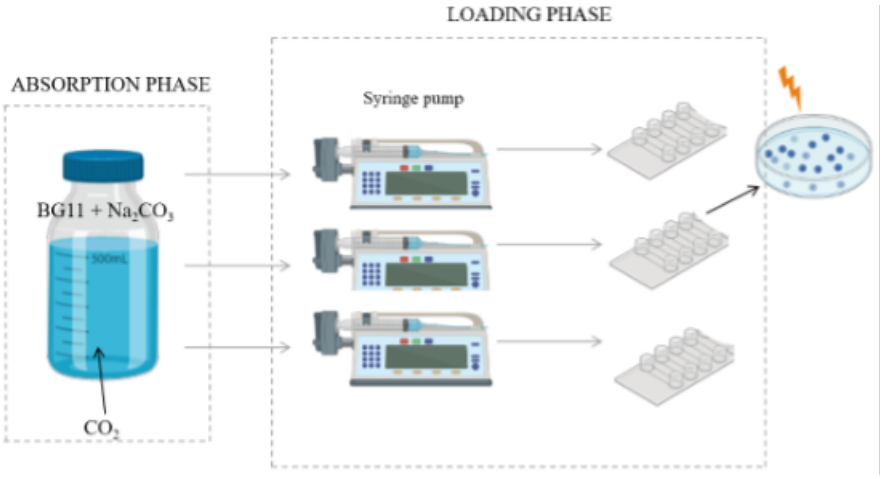


Figure 2.5 Adsorption and loading phase for microalgae cultivation in microchambers. [6, 86]

2.3.2 Microalgal Separation Process

Microalgae have high photosynthetic rates and may produce an abundance of biomass if conditions are optimized adequately [88]. Following the cultivation processes, the process requires several downstream operations such as harvesting, extraction, pretreatment, and purification to obtain biomass or the final product [89]. Also the majority of microalgal bioprocess and biotechnology applications, it should be made sure that microalgal growth should be uncontaminated with bacteria and other microorganisms in order to ensure reproducibility of experiments and production, high-end product and biomass quality, scaling-up and research validity. While sedimentation, flocculation, centrifugation, and filtration are commonly used to separate biomass and supernatant in a pure microalgae culture, conventional methods such as antibiotic or lysozyme treatment and serial dilution are generally used for microalgae isolation and separation from other contaminants [90–93].

The design of microfluidic devices for microalgae separation emerged as one of the most popular recent research subjects, as the conventional methods of separation and purification are usually time-consuming, low-efficient, energy-intensive, and costly. Microfluidic systems enable process-specific microchannel or system design. Due to their automatic control, there are more control over the process, more reliability in the outcomes, fewer human error opportunities, and enhanced process efficiency through the integration of microfluidic devices with cultivation. In comparison to earlier approaches, a variety of portable microfluidic techniques have recently been developed to detect the differences in the size, shape, and content of cells. These techniques are low-cost, high-throughput, and very sensitive, and they require a significantly less amount of inoculum and reagents [94, 95]. Several methods for rapidly and constantly isolating and separating cells have been

developed using the distinctive characteristics of microfluidic devices [96].

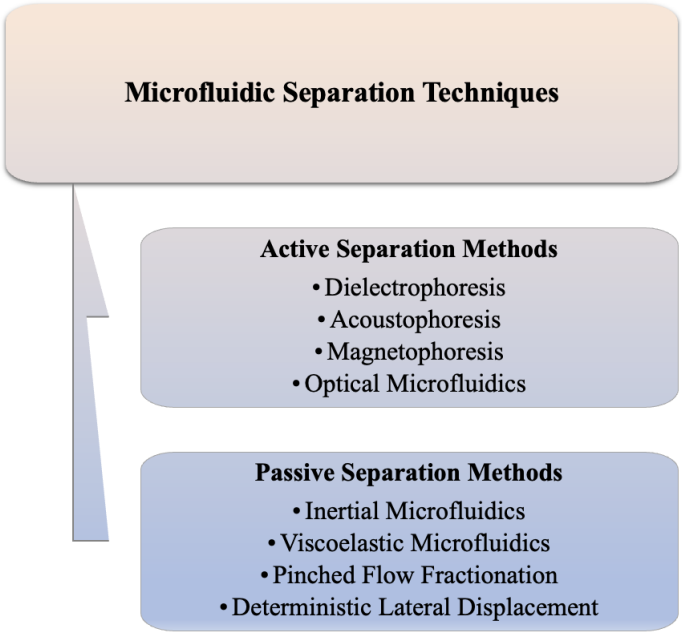


Figure 2.6 Microfluidic separation techniques

Figure 2.6 illustrates the two main classifications of microfluidic systems for separation techniques—passive and active methods—depending on the presence or absence of external force and the methods are classified according to their operating characteristics. Active techniques employ external forces such as electric, magnetic, and acoustic forces, whereas passive methods primarily rely on hydrodynamic forces as well as the size and morphology of the cells, which is an advantage for passive systems [96, 97]. Active separation methods offer higher particle separation efficiency than passive separation techniques, despite the benefits of passive methods. Relevant research focuses on the use of these techniques either individually [90] or in combination [95] to benefit from the advantages of two separation methods. Because it could be difficult to employ a single device with high sensitivity and a wide operating range to separate biological samples containing a large number of cells, such as blood [98].

The literature review on microalgae isolation and separation processes includes research for both passive and active approaches; however, as it is unclear how the external stimuli utilized in active methods would affect the cell, most studies have considered passive methods.

2.3.2.1 Active Techniques for Microalgae Separation

Active separation methods include dielectrophoresis based on electrical properties, magnetophoresis based on magnetic force, acoustophoresis based on acoustic waves, and optical microfluidics based on light sources such as lasers as illustrated in Figure 2.7 [6, 99].

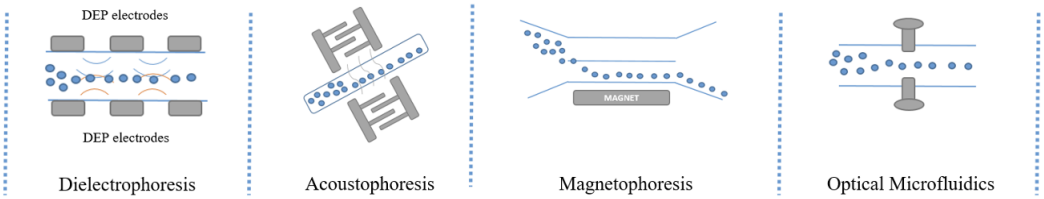


Figure 2.7 Active separation methods in microfluidics [6]

A microfluidic device based on dielectrophoresis (DEP) was suggested in one research as an approach to detecting microalgae cells in ballast water and separating them from contaminants. Sheat flow was applied for higher DEP force to the microalgae cells, and the microchannel has constructed in an insulated triangle with three-dimensional electrodes in order to assure the separation process in this microfluidic system [100]. In another study, separation of *Chlorella* cells was achieved by combining liquid-liquid fractionation, known as aqueous two-phase system (ATPS), with microfluidics based on electrical forces. In ATPS, a liquid-liquid interface that acted as a filter was created within microchannels, and polyethylene glycol and dextran were used to create two phases. Microalgae were able to migrate across the liquid-liquid interface by regulated electrophoretic mobility, which enabled the separation process [101].

Alternatively, DEP-based microfluidics was utilized to identify and separate the microalgae with the highest lipid content since the varying lipid contents of the microalgae cells exhibited differences in their dielectric characteristics, including differences in the conductivity of the cytoplasm as can be seen in Figure 2.8 [102].

The issues under investigation also include how various lipid concentrations and sizes of microalgae impact the separation process, if the separation processes differ from one another, and how they interact with one another. *Crypthecodinium cohnii* were separated in a DEP-based microfluidic system developed for this purpose, and *in situ* analysis was performed using a fluorescent microscope to observe cell movement and cells with a different lipid content. It was found that large-sized cells were oriented in the microchannel by being exposed to the DEP force, but small-sized cells were separated mostly according to the change in lipid content [103].

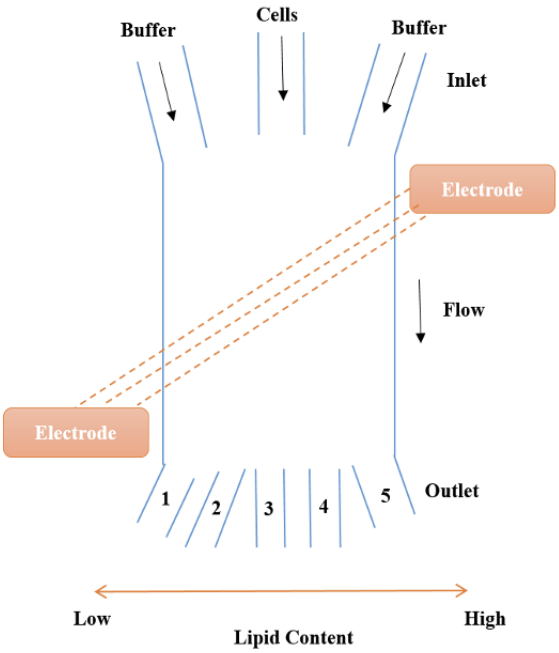


Figure 2.8 Lateral DEP-based microfluidic device to detect the microalgae with highest lipid content [6, 102]

2.3.2.2 Passive Techniques for Microalgae Separation

Passive separation techniques in microfluidic systems rely on the shape of the channels, forces exerted by the movement of fluids, and physical properties of cells or particles. These techniques have several advantages over active separation methods, including absence of external power, easy operation, and minimized stress on the cells. Additionally, passive separation systems generally achieve high efficiency. The efficiency of separation in passive techniques is greatly influenced by the design of the microchannels. By manipulating the movement of algal cells, the microchannel design could utilize centripetal and centrifugal forces to separate other particles from the surrounding environment as mentioned in Figure 2.9 which represents different techniques in the passive separation methods.

Separation based on the particle size depends on the inertial and Dean drag forces that occur in curved microchannels. These forces create a secondary flow pattern known as Dean flow, which results from differences in velocity and generates a radial pressure gradient that helps push the fluid components outwards [104–107]. More clearly, particles of larger size will come into contact with more significant buoyancy, resulting in their proximity to the inner wall of the microchannel. Conversely, particles of smaller size will deal with a stronger Dean drag force, which makes them closer to the outer wall [108].

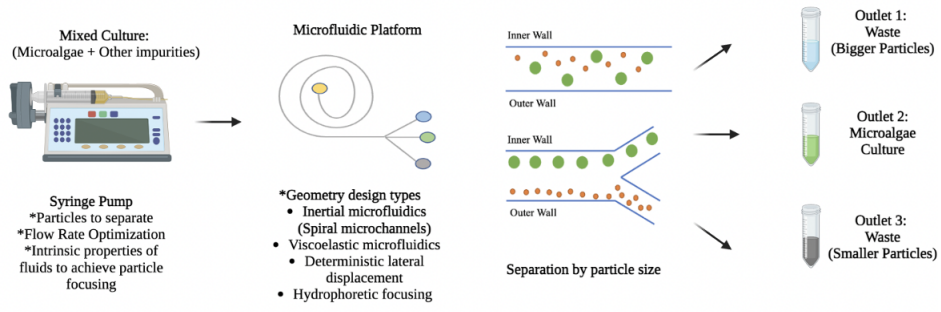


Figure 2.9 Passive separation methods in microfluidics [6]

Some researchers identified various passive techniques and microchannel configurations for separating microalgae. The related research involved modifying the geometries of the output channels, adjusting the number of output channels, and varying the number of cycles based on inertial forces. *Scenedesmus dimorphous* was harvested using spiral microchannels [109], while *Euglena gracilis* was harvested using flat rectangular microchannels [110]. Preferentially, spiral channels were utilized to isolate *Tetraselmis suecica* from *Phaeodactylum tricornutum* [90, 106]. Inertial forces were utilized to separate *C. vulgaris* from *atococcus pluvialis* [111]. In the context of a more complex system, inertial forces and dielectric characteristics were employed to separate cells of varying sizes within a culture containing *Chlorella*, *Platymonas*, and *Closterium* [95]. Inertial forces were employed to separate *C. reinhardtii* [112] and *Coenochloris signiensis* from bacteria [10].

The deterministic lateral displacement method, a passive separation approach, is employed to separate particles based on their diameter relative to the critical diameter. This method was also implemented in the literature for the separation of microalgae [113, 114]. Y. Wang et al. [115] designed microfluidic chips featuring two distinct micro-shapes, triangular and circular which aimed at enriching and purifying microalgae *Platymonas* cells. The chip has equipped with two inlets, one for the sample and one for the sheath, as well as two outputs. These outlets were used to separate the zones for Platymonas cells and waste. The purpose of the sheath intake was to provide hydrodynamic resistance, which effectively prevented the diffusion of small particles into the center enrichment zone.

The pinched flow fractionation (PFF) microfluidic method utilized laminar flow to continuously separate particles based on their size. In a PFF device, a guiding flow directed the particle-containing flow to the sidewall in a restricted region known as the pinched region. To achieve this, particles of varying sizes are initially focused against one sidewall of a microchannel using a strong sheath

flow induced by pressure or an electric field. However, PFF typically operates at higher flow rates, and the separation distance in the expanding portion was limited. To enhance the separation efficiency of PFF, the inertia-enhanced pinched flow fractionation (iPFF) method was developed [116–118]. S. Wang et al. [119] applied iPFF to separate microalgae of different sizes and to detect microalgae in ballast water. In the microfluidic chip designed using iPFF, there were two inlets for the microalgae mixture (*Tetraselmis* sp. + *Chlorella* sp.) and deionized water sheath flow. Deionized water was introduced before the microalgae mixture to prevent the microalgae from entering the sheath fluid channel. The microalgae mixture was initially focused on one sidewall of the T-shaped channel with a sheath fluid flow and then propelled towards the channel center by the inertial lift force caused by the flow.

A highly useful technology in biology, biochemistry, and medicine involves the generation of hydrogel droplets through droplet microfluidics for encapsulating cells. In this process, uniform water droplets surrounded by oil could be formed when two immiscible fluids, typically water and oil, intersect in droplet microfluidic devices. Compared to water-in-oil droplets, hydrogel droplets are more stable and easier to manage during subsequent analysis processes, reducing the risk of aggregation [120]. Analysis of the hydrogels of varying sizes revealed the presence of microalgae cells in small hydrogels, while large hydrogels showed absence of microalgae. According to related study, the reason for this lied in the observation that hydrogels of larger size tend to have an average lateral position and are positioned closer to the center. Consequently, small and large hydrogels have distinct equilibrium positions [105]. Lee et al. [108] successfully encapsulated *C. vulgaris* and *Cosmarium* microalgae based on their size disparities. They subsequently devised spiral microchannels to separate hydrogels of varying sizes.

Viscoelastic microfluidic techniques were employed to focus particles of small sizes, to enhance separation efficiency, and mitigate the constraints imposed by the growing influence of Brownian motion at decreasing particle sizes. Nevertheless, this approach is constrained by the requirement for greater pressure and higher viscosity [121, 122]. In the study by Yuan et al. [123] a microfluidic platform that effectively separated and purified microalgae *Chlorella* from bacteria *Bacillus subtilis* was designed and developed. The platform consisted of one inlet and three exits and took advantage of the viscoelastic features of the medium to achieve continuous separation. This research represents a notable breakthrough by introducing the initial viscoelastic microfluidic technique for the continuous separation of microalgae and bacteria which eliminate the requirement for a sheath flow. In order to accomplish optimal separation and purification, a minute quantity

of a biocompatible polymer was added to the microalgae-inlet medium that was contaminated with bacteria. Using size-based differential viscoelastic focusing, the migration of bigger microalgae cells was observed towards the walls of the channel, while small bacteria were observed to move towards the middle of the channel.

2.3.2.3 Pretreatment and extraction

Several methods are available to obtain valuable substances from microalgae, which could be located within the cells, outside the cells, or in the periplasmic space. In order to maximize the retrieval of valuable products, it is critical to integrate these methodologies to the related application while minimizing costs, energy usage, and chemical inputs. Conventional approaches, while successful, frequently demonstrate substantial discrepancies in rates of recovery and require substantial investments of labor, time, devices, and financial investment. As a result, there is an increasing need for innovative and alternative approaches. Considering the drawbacks of traditional techniques, microfluidic systems emerge as a potential solution for downstream pretreatment and extraction processes. In addition to the inherent benefits of microfluidic devices, this system allows for a combination of pretreatment and extraction operations into a single device, thereby permitting a rapid and efficient operation that optimizes resources [124–126].

Various investigations were made regarding the astaxanthin production and the extraction of astaxanthin using microfluidic technologies. Yao et al. [127] performed an experimental study and they stimulated the accumulation of astaxanthin in *H. pluvialis* cells by using micropillar arrays. They then cultivated the cells on a microfluidic platform and observed the cells transitioning from the vegetative phase to the cystic phase. Cheng et al. [128] employed parallel cell traps to gather *H. pluvialis* cells, subsequently subjected them to high pressure and high temperature to rupture the cell wall, and finally extracted astaxanthin using solvent extraction as showed in Figure 2.10. Similarly, Cheng et al. [11] utilized C-shaped traps for trapping *H. pluvialis* cells and acquired astaxanthin using supercritical CO_2 extraction after employing a hydrothermal method.

Currently, algae has been mostly utilized in the production of biodiesel because of its abundant lipid content while the development of this technology is challenging [129]. The literature currently lacks a straightforward and cost-effective microfluidic device for rapid and efficient screening and analysis of the entire process, from microalgae cultivation to lipid extraction, as well as achieving high lipid productivity in different microalgae strains. Lim et al. [124] and Kwak et al. [130] employed comparable microfluidic devices to carry out strain scanning in

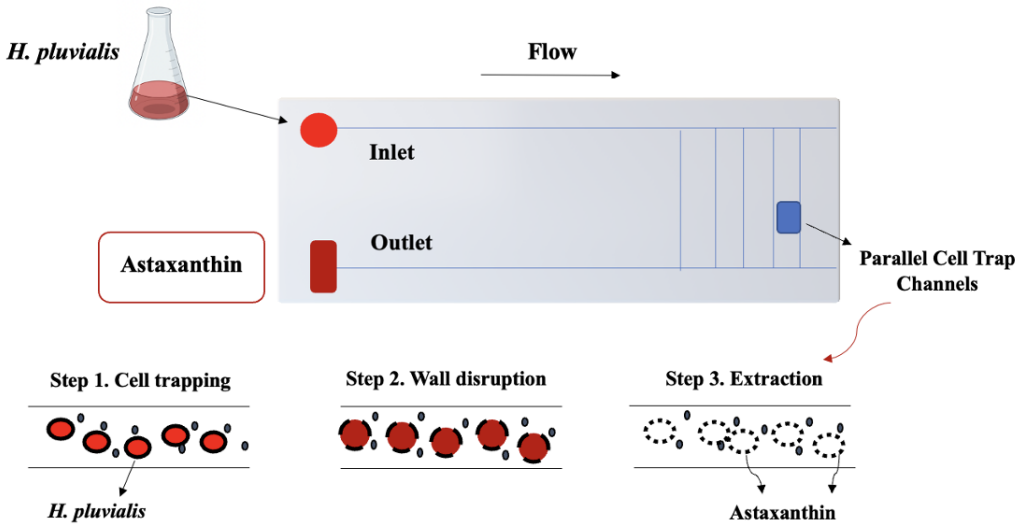


Figure 2.10 Astaxanthin accumulation in microfluidic platform [6, 128]

order to optimize lipid productivity. The upper section of the microfluidic platform, comprising two layers, served as a filter for the cells and retained the cell pellet during lipid extraction. The lower part contained the cell chamber and outlet reservoirs. Media lacking nitrogen have been employed to enhance the amount of lipids. Subsequently, the microfluidic platforms were positioned on the heated plate and the process of solvent extraction was carried out. Lim et al. conducted a screening of *C. reinhardtii* strains CC503, CC124, and CC4348, whereas Kwak et al. focused on *C. reinhardtii* strains CC124, CC125, and CC4348, as well as *C. vulgaris*, *C. protothecoides*, *Neochloris oleoabundans*, *C. zofingiensis*, and *Scenedesmus* sp.. Microalgae can be meticulously selected through strain screening to enable large-scale production which can result in the development of the most effective process for biodiesel generation (Figure 2.11).

2.3.3 Microfluidic Devices as Algal Biosensor

The integration of microalgae biotechnology and biosensors offers the possibility for highly sensitive, long-lasting, and versatile detection. Their application areas are extensive due to their synergistic utilization with various technologies. Algae-based biosensors need to demonstrate high sensitivity and stability, which are of utmost importance. Algae cultures frequently necessitate specific conditions of salinity, temperature, and light [102]. A microfluidic chip that could detect chlorophyll in the surrounding environment [131] could identify the presence of microalgae in ballast water. Furthermore, some researchers utilized the chip to examine the effect of specific chemicals on chlorophyll production [12]. Furthermore, they investigated the difference in capacitance between living microalgae and

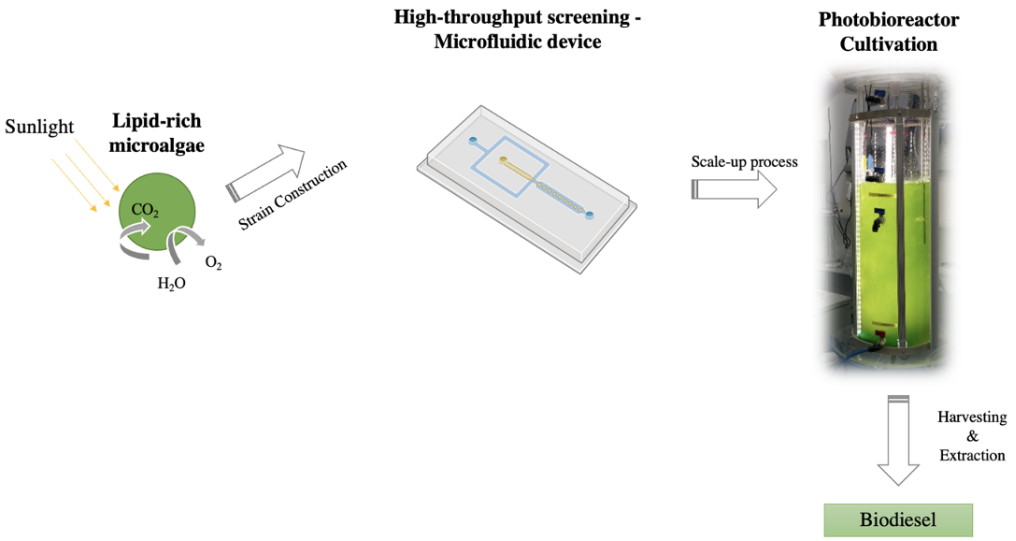


Figure 2.11 High-throughput screening for microalgal strains in microfluidic platform [6]

dead microalgae. A novel biosensor was engineered to specifically identify viable microalgae while considering their inherent variations [132]. In a separate research effort, the microfluidic diatomite analysis instrument detected both the pollutants in wastewater and metabolites generated by diatoms. The impact of algae concentration and light intensity on pollution levels was investigated and the disruptions to photosynthesis were examined. Utilizing a combination of cutting-edge technologies and microfluidic chips, the detection was successful [13]. The process of isolating individual cells from *Dunaliella salina* and *Tetraselmis chui* was carried out utilizing a bubble surface technique using a microfluidic chip with flat microchannels [133].

3
MATERIALS AND METHODS

This thesis initially involved the use of microfluidic systems to separate microalgae from bacteria, followed by the application of antimicrobial agents to a mixed culture of microalgae and bacteria for comparison with the conventional method. Following the separation procedures, the microalgae and bacteria were quantified, and the efficiency of the separation was assessed.

Regarding the separation procedures utilizing the microfluidic system, each trial of the microfluidic system lasted for a duration of 4 days. This duration consisted of 1 day dedicated to the manufacture of the microfluidic system, 2 days allocated for the application and analysis of the experiments, and 1 day designated for the reception of the analysis results. Each trial of antibiotic application for microalgae cultivation lasted for a total of 16 days, consisting of 15 days for the experiment application and analysis and 1 day for receiving the analysis results. A minimum of three repeats were performed for each experimental set.

3.1 Determination of Microorganism Sizes in Samples from Antarctica and Microorganism Selection

A light microscope (Olympus CX22 Binocular LED Microscope) was used to examine a liquid sample that had been collected from TAE-III and utilized for recognizing species. Microalgae are green, and bigger microorganisms can be seen with a light microscope. To make small bacteria visible, gram staining (Gram Staining Kit, Merck) was used in the Yıldız Technical University Algal Biotechnology and Bioprocess Laboratory. The steps for gram staining are shown in Table 3.1. To perform Gram staining, a liquid sample obtained from the samples collected in Antarctica was withdrawn using a Pastor pipette and poured onto a slide. The samples were quickly heated in order to fix them onto the slide and prepare them for further staining. In order to observe the samples, photographs were captured using a light microscope at a magnification of 100X. The microalgae

and bacteria were observed through a microscope, and their sizes were determined using the Image J program [134, 135].

Table 3.1 Gram staining steps

Component	Duration	Reason
Crystal Violet	1 min	All bacteria are stained, but the peptidoglycan in Gram-positive bacteria adheres to the dye.
Lugol Solution	rinse briefly	For the dye to adhere
Lugol Solution	1 min	For the dye to adhere
Distilled Water	5 sec	Washing
Ethyl Alcohol	10-15 sec	Decolourization step. Alcohol dissolves the lipids in the outer membrane of gram-negative bacteria; pores open, and crystal violet is dispersed.
Distilled Water	5 sec	Washing
Safranine	1 min	To stain gram negative bacteria
Distilled Water	5 sec	Washing
Air-dry	10 min	50°C in the drying cabinet

3.2 Microorganism Cultivation

3.2.1 Selecting Microorganisms to Assess Separation Performance

The microalgae *Chlorella minutissima*, The Culture Collection of Algae at the University of Göttingen, Germany, obtained from the Algal Biotechnology and Bioprocess Laboratory of Yıldız Technical University, Türkiye, were chosen as a model to assess the effectiveness of microfluidic platforms that will be designed based on the average sizes of microalgae in Antarctic samples, as determined via the Image J program.

The bacteria *Escherichia coli* ATCC 25922, obtained from the Algal Biotechnology and Bioprocess Laboratory of Yıldız Technical University, Turkey, were chosen as a model to assess the effectiveness of microfluidic platforms that will be designed based on the average sizes of bacteria in Antarctic samples, as determined via the Image J program.

The selection of this species as based on a limited amount of samples obtained from Antarctica, significant research was carried out with *C. minutissima* in the Algal Bioprocess and Biotechnology Laboratory, and stock cultures of *C. minutissima* and *E. coli* are available.

3.2.2 Microalgae Cultivation

The microalgae were cultivated in 250-mL Erlenmeyer flasks, with a volume of 150 mL. For the experiment, 10 mL of stock *C. minutissima* culture, 3 mL of Bold Basal Medium (BBM) as a nutrient medium, and 87 mL of DW were mixed in Erlenmeyer flask. The flasks were then placed in a shaking incubator (Kerman brand incubator (Figure 3.1) and incubated at a temperature of 25°C, a light intensity of 8000 lx, continuous illumination, pH=7.2 and a shaking speed of 150 rpm for a duration of 14 days. Simultaneously, microalgae were cultured in petri dishes using BBM medium supplemented with 15 g/L Agar Agar at a temperature of 25°C, a light intensity of 8000 lx and continuous illumination for a duration of 14 days. Prior to the study, all materials were utilized, including DW and BBM, underwent sterilization using an autoclave operating at a temperature of 121°C and a pressure of 1 atm and the experiments were conducted within a laminar flow cabinet (Class II-A2, Mikroair Flow Cabinet, Mikrotest Cihazları).

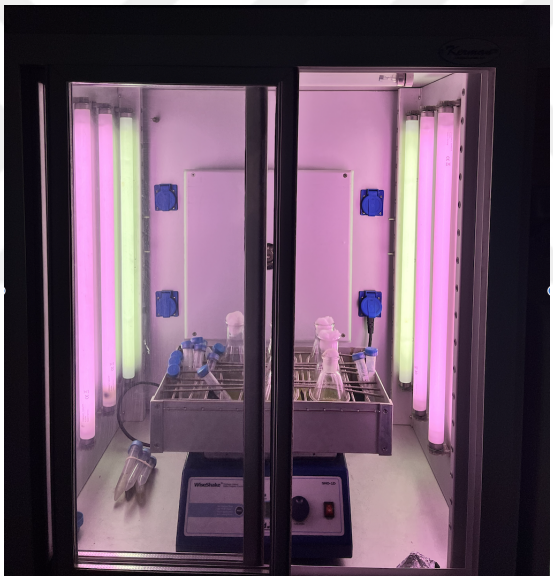


Figure 3.1 Kerman Brand Incubator, Wiseshake orbital shaker

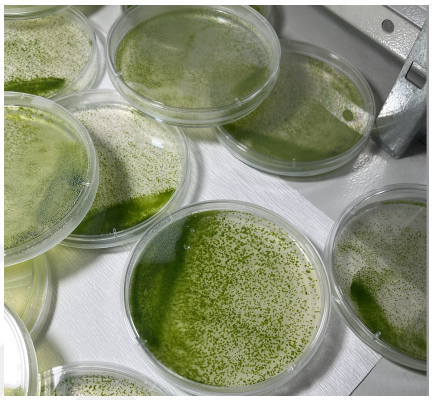
The absorbance was quantified at a wavelength of 680 nm using a UV-Vis spectrophotometer. This measurement was taken periodically over a period of 14 days. *C. minutissima* culture is displayed in Figure 3.2 after 14 days of cultivation. Afterwards, a growth chart of the microalgae was constructed, and the specific growth rate and doubling time were calculated as mentioned in equations 3.1 and 3.2, where $\mathrm{OD_t}$ is the optical density on the final day and $\mathrm{OD_0}$ is the optical density on the first day. Microalgae production was maintained throughout the experiments, and stock cultures were established by placing them in 50-mL centrifuge tubes [75, 136].

$$Growth\ Rate\ (1/day) = lnOD_t \cdot lnOD_0 \tag{3.1}$$

$$Doubling\ Time\ (day) = \frac{ln2}{Growth\ Rate} \tag{3.2}$$



(a) *C. minutissima* culture in erlenmeyer



(b) *C. minutissima* culture in petri dishes

Figure 3.2 *C. minutissima* cultures

3.2.3 Bacteria Cultivation

The bacteria were cultured in sterile glass bottles with a working volume of 10 mL. Nutrient Broth (NB) (8 g NB: 1 L DW) was formulated and autoclaved at 121°C, 1 atm pressure, in preparation for bacterial inoculation. Following the sterilization process, NB was permitted to cool to the ambient temperature. Thereafter, samples were collected from the stock *E. coli* cultures in solid agar using sterile plastic inoculating loops and then introduced into NB at the ambient temperature. The tests were done adjacent to the burner flame. The bacteria were cultured at a temperature of 37°C for a duration of 24 hours. After 24 hours, the absorbance of the bacterial solution was quantified at a wavelength of 600 nm using a UV-Vis spectrophotometer. *E. coli* culture is demonstrated in Figure 3.3 after 24 hours of inoculation [137].

A solution of Nutrient Agar (NA) was prepared by dissolving 20 grams of NA in 1 L of DW. The solution was then sterilized using an autoclave at a temperature of 121°C and 1 atm. This sterilization process was necessary to prevent the presence of bacteria and to facilitate accurate colony counting when obtaining stock cultures and performing separation procedures. Following sterilization, the NA solution was cooled to a temperature range of 60–70 °C. Subsequently, the sterile petri dishes

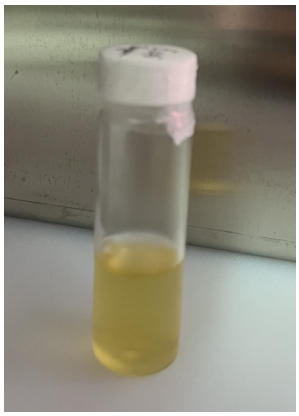


Figure 3.3 *E. coli* after 24-hours incubation

were filled with the NA medium in a laminar flow cabinet. The petri dishes were then left to cool down to room temperature. The solid media were covered with parafilm and stored at a temperature of +4°C [138].

3.3 Design and Microfabrication of Microfluidic Platforms

Prior to the development of microfluidic platforms, fluid mechanics-related calculations were performed to asses the ranges of major parameters. Drag force ($\mathrm{F_D}$), Dean (De), and Reynolds (Re) numbers were found according to the equations 3.3, 3.4, 3.5, and 3.6 below [68, 139].

$$D_h\ (m) = \frac{2(a * b)}{a + b} \tag{3.3}$$

$$U_f\ (m/s) = \frac{Q}{A} \tag{3.4}$$

$$F_D = 3\pi\mu U_{De}\alpha_P \tag{3.5}$$

$$U_{De} = 1.8 \cdot 10^{-4} \cdot De^{1.63} \tag{3.6}$$

$$De = (\frac{\rho_f U_f D_h}{\mu}) \cdot \sqrt{(\frac{D_h}{2R})} = Re \cdot \sqrt{(\frac{D_h}{2R})} \tag{3.7}$$

$$Re = (\frac{\rho_f U_f D_h}{\mu}) \tag{3.8}$$

Prior to utilizing equations 3.5-3.8, the values of $\mathrm{D_h}$ and $\mathrm{U_f}$ were calculated. $\mathrm{D_h}$ was calculated which a is channel height (100 μm) and b is channel width (500 μm), while $\mathrm{U_f}$ was determined using equation 4.2 which Q is flow rate and A is cross-sectional area. Since $\mathrm{D_h}$, channel height and channel width are the same on all platforms, it is constant for all platforms and is calculated as 0.00017. The values of $\mathrm{U_f}$ vary for each of the five flow rates, and the corresponding outcomes

Table 3.2 Design parameters of microfluidic platforms for microalgae separation

Microfluidic Platform	**A**	**B**	**C**	**D**	**E**
Type of Microchannel	Spiral	Spiral	Spiral	Spiral	Spiral
Height of Microchannel	100 µm	100 µm	100 µm	100 µm	100 µm
Width of Microchannel	500 µm	500 µm	500 µm	500 µm	500 µm
Number of turns	3	5	7	5	7
Distance Between turns	2 cm	2 cm	2 cm	6 cm	6 cm

are presented in Table 4.1.

The AUTOCAD software (2018) was utilized to design a distinctive microfluidic platform that is adequate for the separation of microalgae from bacteria. The microfluidic platforms were designed in a 2D format and feature spiral microchannels. To achieve this, five different microchip designs were considered by altering the number of cycles and the distance between turns. The specifications for microfluidic design parameters are provided in Table 3.2. Apart from this, in the microchannel geometry, the channel width was kept constant is 500 μm while the channel height is 100 μm, the inner diameter of the entrance channel was 2 cm and the radius of curvature is 4 cm. The 2D designs developed for microfabrication were used to prepare lithography masks. The service procurement was acquired for the printing of photomasks on acetate sheets from Çözüm Merkezi, Ankara, Turkey.

The fabrication of microfluidic platforms based on PDMS molding followed the standard soft lithography method, with the materials and equipments specified as seen in Table 3.3 and Table 3.4, respectively [68, 140].

1. The microfabrication steps of PDMS-based microfluidics were carried out under clean-room conditions at Sabancı University Nanotechnology Research and Application Center (SUNUM).

2. Cleaning of silicon wafers (University Wafer, Inc., Boston, MA, USA): The silicon wafers intended for use went a cleaning process involving acetone, isopropyl alcohol (IPA), and DW.

3. For the PR-Su-8 3050 photoresist (Microchem Corp., Westborough, MA, USA) coating, the silicon wafers that had been previously cleaned were

Table 3.3 Materials for microfabrication steps

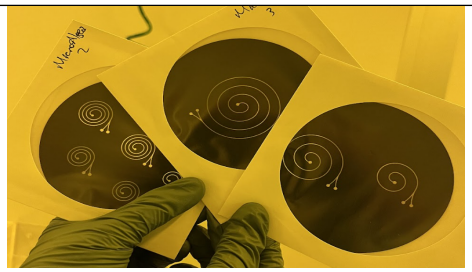
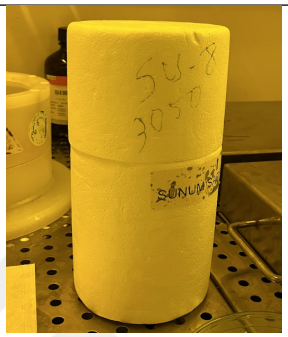
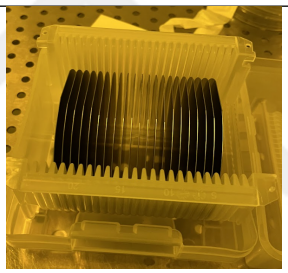
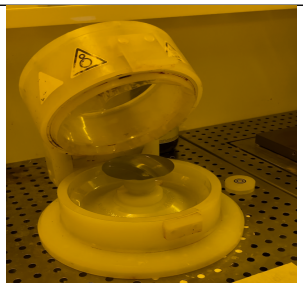
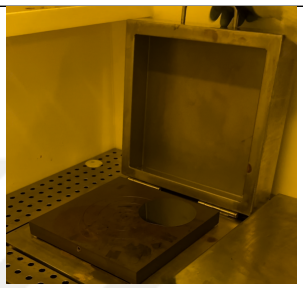
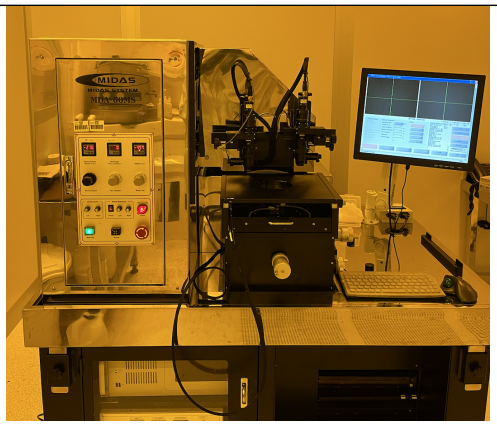
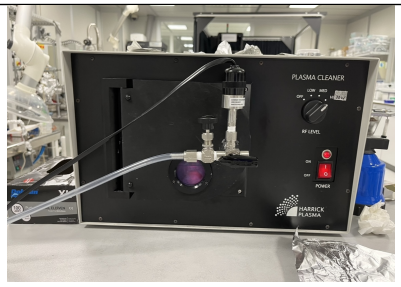
Materials	Figures
Acetate Sheets	
SU-8 Negative Photoresist	
Silicone Wafers	
Acetone	
Isopropyl Alcohol	
Distilled Water	
SYLGARD™ 184 Silicone Elastomer Kit	
Glass Petri	
Glass Slide	
Thermal Tape	
Magnetic Stirrer Fish	
21-gauge needle	

Table 3.4 Equipment for microfabrication steps

Equipments	Figures
SPS Spin 150 for coating photoresist	
Heater	
Oven	
Mask Aligner UV-Lithography	
Oxygen Plasma Cleaner	
Magnetic Stirrer	

inserted into the SPS Spin 150 device as demonstrated in Figure 3.4. The coating procedure was divided into two phases. Silicon wafers were coated with Su-8 3050 negative photoresist. Vacuuming and heating the wafers were carried out.

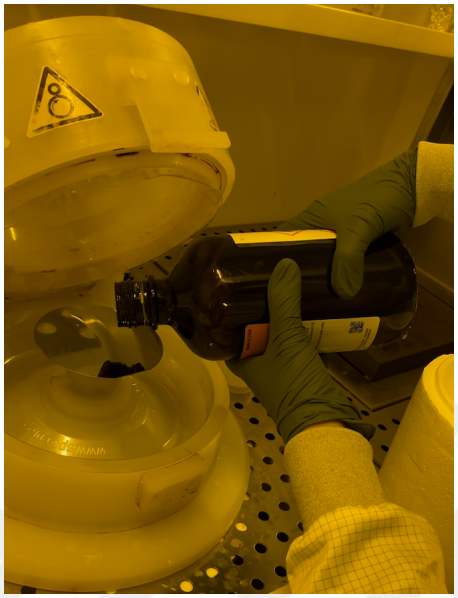


Figure 3.4 Silicon wafer coating process with PR-Su-8 3050 photoresist

4. The glass petri dishes were cleansed using IPA and then dried with nitrogen gas. The acetate sheet was affixed to the glass petri dish with thermal tape.

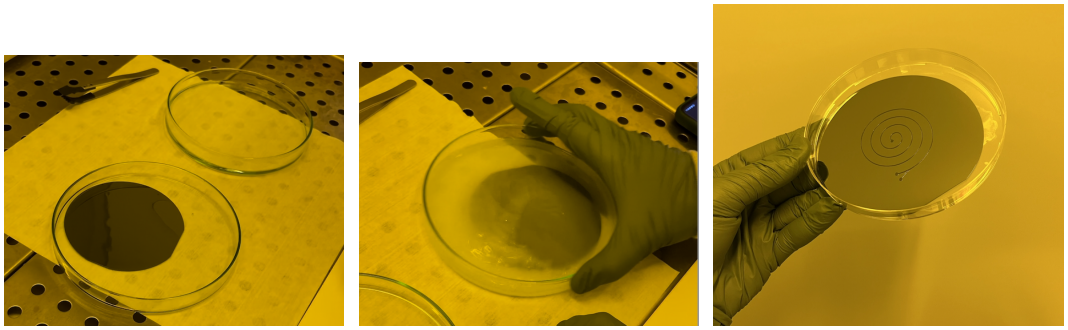
5. The glass petri dish with photomask and baked silicon wafers were placed and aligned in the Mask Aligner UV-Lithography device (Midas System Co., Ltd., Daejeon, Korea, MDA-60MS Mask Aligner 4") for UV exposure. The silicon wafers were vacuumed, and then patterns were applied.

6. The molds were baked separately, with the front and back parts, at a temperature of 65°C and 95°C, for a duration of 5 minutes, respectively.

7. The SU-8 developer were dispensed into glass petri dishes. The baked silicon wafers are immersed in SU-8 developer and agitated continuously for around 10 minutes. Subsequently, the presence of microchannels became apparent as the regions unaffected by UV light were dissolved by the developer. SU-8 development steps are shown in Figure 3.5.

8. Silicon wafers had an IPA wash to remove impurities, followed by stopping the reaction and drying using nitrogen gas.

9. The shape and structure of the microchannels were examined using a light microscope.



(a) Beginning of the development

(b) Development

(c) Silicon wafer after development

Figure 3.5 Development process

10. To prepare PDMS, a mixture of 100:1 silicone elastomer base and curing agent (from SYLGARD™ 184 Silicone Elastomer Kit) was stirred for 10 minutes and subsequently subjected to vacuuming to eliminate any foams present in the mixture for 2 hours (Figure 3.6).



Figure 3.6 Vacuuming of PDMS

11. The wafers that had been prepared were affixed to the petri dishes using a tape. The wafers were coated with PDMS (Figure 3.7). Subsequently, the wafers underwent a baking process in an oven heated to a temperature of 75°C for a duration of 2 hours.

12. The PDMS was removed from the cured molds, and the PDMS microchannels were purified.

13. The glass slide and PDMS microchannels were adhered together, and their surfaces were treated with oxygen plasma in a Harrick Plasma Cleaner device located in Ithaca, NY, USA.

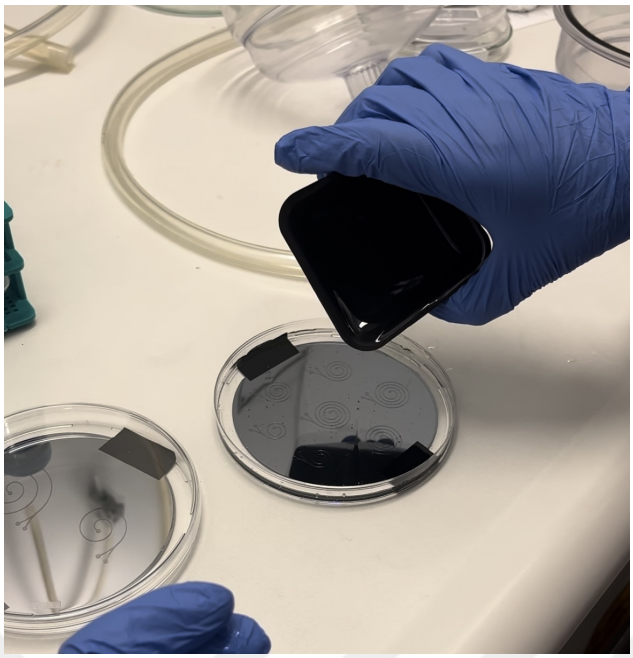


Figure 3.7 Silicon wafer coated by PDMS

14. In order to ensure a permanent connection, the processed surfaces were compressed, and spiral microchannel structures were developed (Figure 3.8).



Figure 3.8 PDMS microchannels after oxygen plasma bonding

15. The microchannels of the microfluidic devices were examined, as evidenced in Figure 3.9 by light microscopy.

16. The inlet and output holes were formed by puncturing with a 21-gauge needle that had sharpened tips.



Figure 3.9 A cross-sectional image of PDMS microchannels under a light microscope

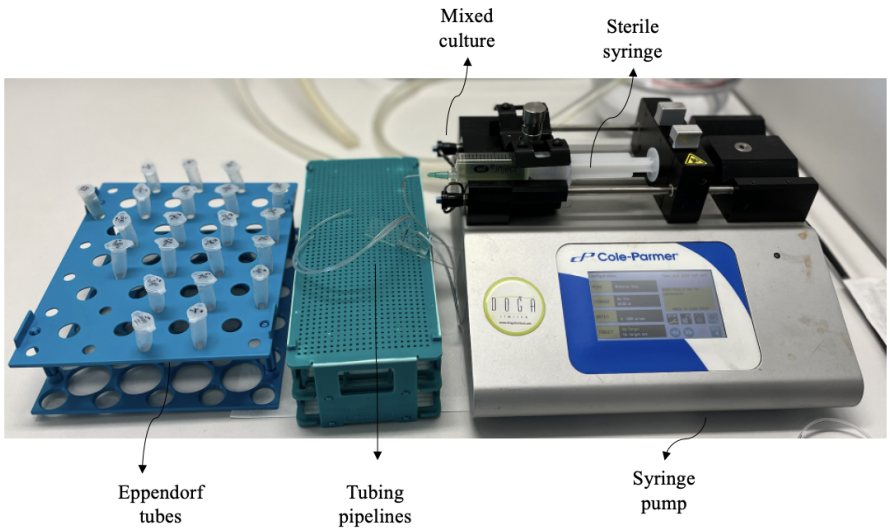
3.4 Experimental Set-up with Microfluidics as A Novel Technology

3.4.1 Preliminary Preparation

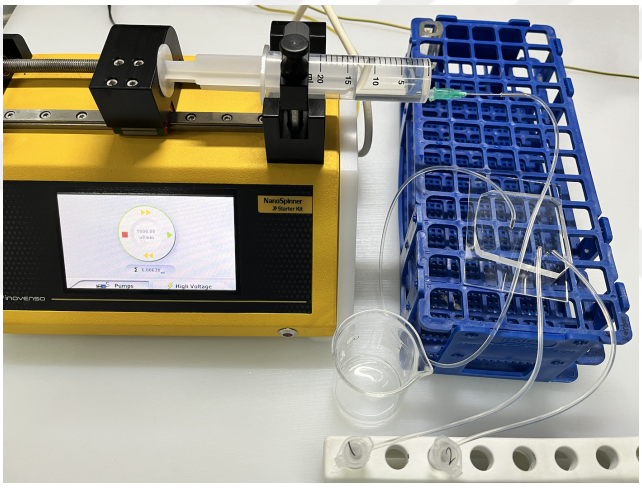
A total of 14 mL samples containing microalgae were taken from the stock cultures and cultivated *C. minutissima* microalgae. These samples then were added to 250-mL Schott bottles. The *E. coli* cell number was adjusted to 0.5 McFarland standard value via dilutions; 1 mL of bacteria samples were then added to 250 mL Schott bottles. A mixed culture was acquired by increasing the working volume by 125 mL of sterile DW to a total of 140 mL. The mixed culture that has obtained comprised cell number in a proportion of 1:1. In order to inhibit bacterial and microalgal growth throughout the experiments, nutrient medium was refrained from being added to the sample, and the Schott bottle containing the mixed culture was maintained at a temperature of +4°C.

After the mixed culture was prepared, five distinct microfluidic chip platforms fabricated at the Sabancı University Nanotechnology Research and Application Center (SUNUM) were utilized to have the experimental setups. They were evaluated at both the "Yıldız Technical University Algal Biotechnology and Bioprocess Laboratory" and the "Microfluidics and Microthermal Systems Laboratory" of the Sabancı University Nanotechnology Research and Application Center (SUNUM).

The microfabricated PDMS microchannels were initially filled with 70% ethanol, followed by sterile DW. In order to prepare the microfluidic chips for the experiment, the tubing and connections were initially connected. Thereafter, fittings



(a) Experimental setup at Sabancı University



(b) Experimental setup at Yıldız Technical University

Figure 3.10 Microfluidic experimental set-up

were utilized to connect tubing pipelines to the outlet channels of the microfluidic platforms. At the beginning of experiments, the mixed culture was filled into a sterile syringe. The syringe was then placed into the syringe pump (Inovenso, Nanospinner Starter Kit; Cole-Parmer Syringe Pump). As depicted in Figure 3.10, the sterile syringe tip was connected via tubing pipelines to the inlet channel of the microfluidic platform, thereby completing the assembly of the system. Experimental preparation stages were carried out in the cabin.

3.4.2 Separation Process Experiments Using Microfluidic Method

Sterile eppendorf tubes were connected to the outlet channels to collect samples from each outlet channel in the microfluidic platforms. The syringe pump was programmed with the desired sample volume and flow rate parameters (1000,

1500, 2000, 2500, and 3000 μL/min, respectively), and the injection was initiated. Samples were obtained from the outlet channels in eppendorf tubes within an exceptionally brief period of time for each flow rate and from each tested microfluidic chip that was microfabricated. The lids of the eppendorf tubes were covered with parafilm and placed at +4°C.

3.4.3 Determination of Separation Performance of Microfluidic Platforms

The separation performance was determined by counting microalgae on a Neubauer slide at the conclusion of the experiments using samples taken from each outflow channel. To determine the mean number of microalgae per milliliter, 16 large squares were counted within each of the four large squares. To find out how many bacteria were there, a sample was taken from each eppendorf tube using an inoculation loop, and the plate count method was used in NA at dilutions of 10^{-1}, $10^{-}3$, and $10^{-}5$. Following a 24-hour incubation period at 37°C, the solid petri dishes were transferred to an oven, and colony counts were conducted at the end of the 24-hour period. In order to find the best microfluidic platform design and flow rate for the separation process, the separation efficiency, separation purity, and enrichment factor were all obtained according to the equations 3.9, 3.10, 3.11 [10, 93, 141].

$$Separation\ Yield\ (\%) = (N_{A_i})/(N_{Total}) * 100 \tag{3.9}$$

$$Separation\ Purity\ (\%) = (N_{A_i})/(N_{Total_i}) * 100 \tag{3.10}$$

$$Enrichment\ Factor = ((N_{A_i})/(N_{Total_i}))/((N_{A_0})/(N_{Total_0})) \tag{3.11}$$

3.4.4 Re-cultivation of Microalgae After Separation Using a Selected Microfluidic Platform

For the separation performance, we passed 50 mL of microalgae+bacteria mixed culture through the selected microfluidic platform using a syringe pump. Centrifuge tubes were used to collect samples from the outlet channel, where microalgae were concentrated, and the waste channel, where bacteria were concentrated. The samples in the channel where microalgae were dense were added to 250 mL conical flasks. 1 mL of BBM and 12 mL of sterile DW were added to the culture medium to make the working volume 50 mL. No antibiotics were added to the culture. The culture was incubated in a shaking incubator at 25°C, 150 rpm shaking speed, and continuous white lighting (approximately 8000 lux) for 10 days. The stock culture was moved to +4°C to determine its biochemical contents [75, 136].

3.5 Experimental Set-up with Antibiotics as A Traditional Method

A total of 14 mL samples containing microalgae were taken from the stock cultures and cultivated *C. minutissima* microalgae. These samples were then added to 250-mL Schott bottles. The *E. coli* cell number was adjusted to 0.5 McFarland standard value via dilutions; 1 mL of bacteria samples were then added to 250 mL Schott bottles. A mixed culture was acquired by increasing the working volume by 125 mL of sterile DW to a total of 140 mL. The mixed culture that is obtained comprises cell number in a proportion of 1:1. Initially, 10 µg of ampicillin antibiotic was introduced into the medium for eliminating bacteria, while 3 mL of BBM was supplemented to the culture medium to facilitate the growth of microalgae. The culture was cultivated in a shaking incubator at a temperature of 25°C, 150 rpm and constant white lighting (about 8000 lux) for a duration of 5 days. Subsequently, a 20 mL volume was extracted from the 5-day-old culture and placed in a medium supplemented with fresh BBM and 30 μg of ampicillin antibiotic. The culture was cultivated in a shaking incubator at a temperature of 25°C, 150 rpm and constant white lighting at about 8000 lux for a duration of 15 days. The stock culture was transferred to a temperature of +4°C in order to analyze its biochemical composition [142].

In order to assess the percentage of culture purity and the efficiency of separation, the microalgal population was quantified using a Neubauer slide. Samples were collected from the culture at three time points: the initial stage, the end of the 5th day, and the end of the 20th day. By counting 16 large squares inside each set of four large squares, it was possible to calculate the average concentration of microalgae per milliliter. In order to quantify the bacteria, a sample was collected from the culture using an inoculation loop and then spread over NA medium at various dilutions: 10^{-1}, 10^{-3}, and 10^{-5}. Subsequently, the solid petri dishes were placed in an oven set at a temperature of 37°C for a duration of 24 hours (Binder, Drying Oven). Following this incubation period, the number of colonies present in the petri dishes was determined. The results were evaluated by comparing them to the microfluidic chip results in terms of separation efficiency and purity according to equations 3.12 and 3.13 [137, 142].

$$Separation\ Yield\ (\%) = (N_{A_final})/(N_{onset}) * 100 \tag{3.12}$$

$$Separation\ Purity\ (\%) = (N_{A_final})/(N_{final}) * 100 \tag{3.13}$$

3.6 Determination of Biochemical Contents After Microalgae Cultivation

A comparison was conducted between *C. minutissima* pure culture, post-chip *C. minutissima* concentrated culture, and antibiotic-treated *C. minutissima* cultures based on the analysis of their carbohydrate, protein, and pigment content.

3.6.1 Phenol-Sulfuric Acid Method for Carbohydrate Determination

To determine the amount of carbohydrates, a stock solution containing 100 mg of glucose per liter was made. Afterwards, glucose solutions with concentrations of 0, 20, 40, 60, 80, and 100 mg per 2 mL were prepared. Following that, a phenol reagent with a concentration of 80% (w/w) was made. 50 μL of phenol reagent and 5 mL of H_2SO_4 were added to the prepared solutions and 2 mL samples, respectively. The solutions were permitted to undergo incubation at ambient temperature for a duration of 15 minutes. The measurement of absorbance was conducted at a wavelength of 490 nm using a UV-Vis spectrophotometer. The standard graph and equation were derived from the glucose solutions, and the glucose concentration in the samples was measured based on this created equation [143].

3.6.2 Protein Analysis (Modified Lowry Method)

A volume of 0.5 mL was taken out of the sample cultures and albumin standards, and then 1 N NaOH was introduced into it. The solution was incubated in a water bath at a temperature of 80°C for a duration of 5 minutes. Reagent C and Reagent D, as indicated in the table 3.5, were introduced to the cooled samples and well stirred. The samples were then subjected to incubation at room temperature for a duration of 30 minutes. After the incubation period, the absorbance was quantified at a wavelength of 750 nm using a UV-Vis spectrophotometer [144].

3.6.3 Spectrophotometric pigment analysis

A volume of 5 mL was taken out of the samples that were stored at a temperature of +4°C. The taken samples were then subjected to centrifugation with a Sigma 2-16KL - Refrigerated benchtop centrifuge at a speed of 8000 revolutions per minute for a duration of 5 minutes. The pellet was treated with acetone, and the acetone samples were mixed thoroughly in an ultrasonic bath (Alex Machine, Ultrasonic Cleaner Machine) for a duration of 10 minutes. The obtained extract was subjected to a second round of centrifugation at a speed of 8000 rpm for a duration

Table 3.5 Reagents prepared for protein analysis

Reagents	Ingredient
Reagent A	5% Na_2CO_3
Reagent B	0.5% $CuSO_4.5H_2O$ in 1% Potassium sodium tartrate
Reagent C	50 mL Reagent A + 2 mL Reagent B
Reagent D	1 N Folin-Ciocalteu (Prepared by diluting 2N Folin reagent at a ratio of 1:1)

of 5 minutes. The liquid portion above the particles, known as the supernatant, was then analyzed for its absorbance values at wavelengths of 666 nm (A_{666}) and 475 nm (A_{475}) using a UV-Vis spectrophotometer, as shown in equations 3.14 [145] and 3.15 [146].

$$Chlorophyll\ a\ (\mu g/mL) = 13.9xA_{666} \tag{3.14}$$

$$Beta\ carotene\ (\mu g/mL) = 4.5xA_{475} \tag{3.15}$$

4
CONCLUSION

4.1 Result and Discussion

4.1.1 Microorganism Sizes in Antarctic Samples

Gram staining results of the samples that were brought from Antarctica with TAE-III, organized by the Ministry of Industry and Technology, the Presidency, and the Istanbul Technical University Polar Research Center in 2019, are shown in Figure 4.1. After performing a size analysis using the Image J software, the average size of polar microalgae was determined to be 7.3 μm, whereas the average size of bacteria was found to be 2 μm. Cell size distribution from Image J is presented in Figure 4.2

Subsequently, in 2019, Antarctic samples were sent to BM Laboratory Systems, Turkey, by the Algal Biotechnology and Bioprocess Laboratory of Yıldız Technical University for the purpose of species identification. Among the samples were microalgae, which included the identification of *Chlorella variabilis* strain YTU.ANTARCTIC.001 and *Auxenochlorella pyrenoidosa* strain Ozcimen.001; additionally, bacteria species like Paracercomonas sp. and amoeba-like Amoebozoa species like *Flamella balnearia*. Communities of microorganisms have been identified in the Antarctic samples with the polymerase chain reaction.

The dimensions obtained using the Image J software for microalgae and bacteria in polar samples are consistent with the information published in the scientific literature. Furthermore, the gram staining reveals a prevalence of pink and purple bacteria and microalgae in the Antarctic sample. Nevertheless, amoebae were not detected in the microscopic image of the sample. After examining the literature, it is clear that the diameter of *Chlorella* sp. typically varies between 1 and 10 microns [147, 148], while the diameter of bacteria often ranges between 0.1 and 3 microns [149]. Amoeba-like microorganisms have been described to have a maximum size of 50 microns, which exceeds the size of microalgae and bacteria [150].

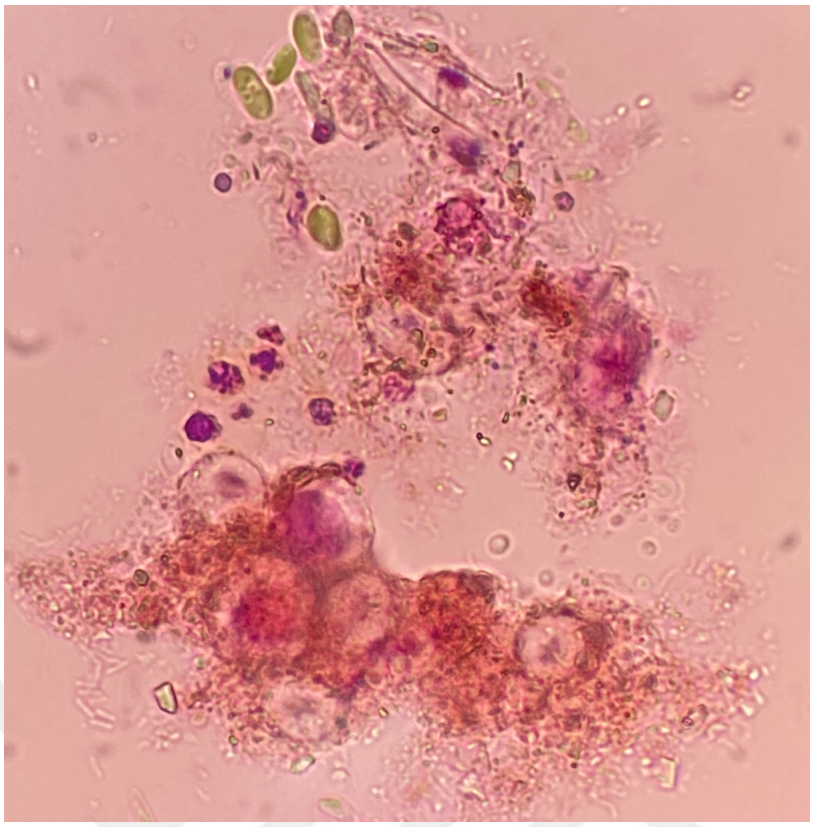


Figure 4.1 Antarctic samples after gram staining under a light microscope at a magnification of 100X

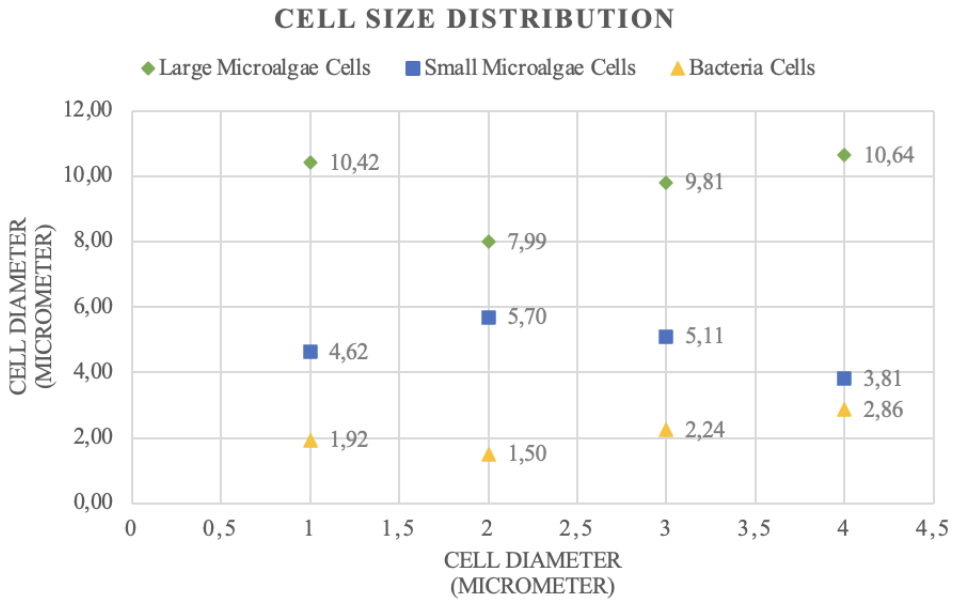


Figure 4.2 Cell size distribution for Antarctic microorganisms

In order to evaluate the effectiveness of microfluidic platforms for separating and enriching microalgae, *Chlorella minutissima* was chosen as the model microalgae, and *Escherichia coli* was selected as the model bacteria, as these microorganisms are prevalent in polar samples.

4.1.2 Microalgae Growth Kinetics

To assess the effectiveness of microfluidic platforms in separating microalgae, absorbance values were measured every day throughout a 12-day cultivation period. The resulting data is presented in Figure 4.3, depicting the proliferation of *C. minutissima* microalgae. Upon completion of the scale-up process, the visual representation of *C. minutissima* cultivated in photobioreactors for a duration of 12 days may be observed in Figure 4.4.

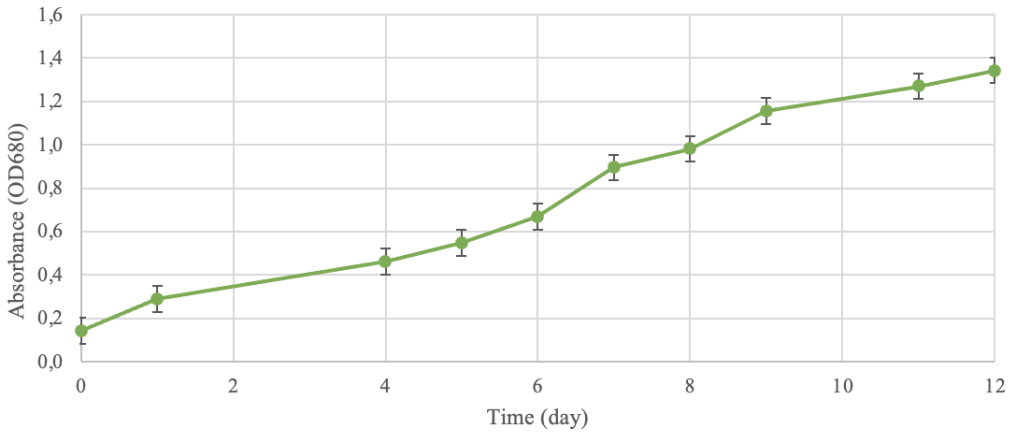


Figure 4.3 Growth kinetics of *Chlorella minutissima*

Based on the Figure 4.3, it was concluded that microalgae were in the adaptation (lag) phase from days 0 to 4, in the logarithmic phase from days 5 to 9, and in the stationary period from days 10 to 12. The specific growth rate and doubling time are calculated based on the logarithmic phase. According to equations 3.1 and 3.2, the growth rate is determined to be 0.1155 day^{-1} and the doubling time is 6 days. Furthermore, Figure 4.5 displays the visual representation of *C. minutissima* during the logarithmic growth phase, as observed using a light microscope at a magnification of 10X.

4.1.3 Design and Microfabrication of Microfluidic Platforms

4.1.3.1 Fluid Mechanics-Related Parameters

The velocity and hydraulic radius were used for calculating the Reynolds number, Dean number, Dean velocity, and drag forces. Spiral microchannels exhibit the

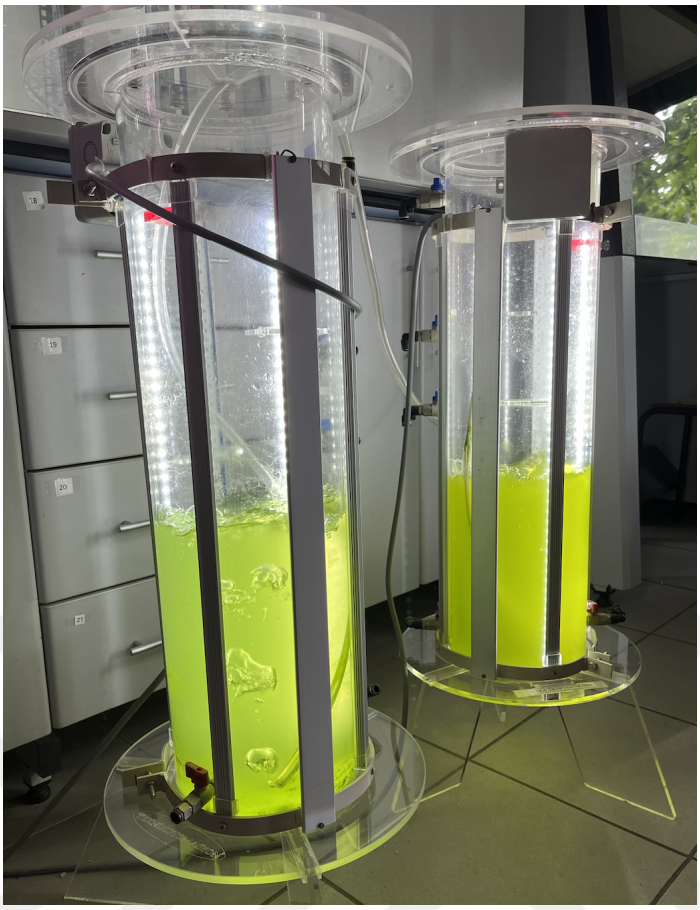


Figure 4.4 *Chlorella minutissima* cultivation in photobioreactor

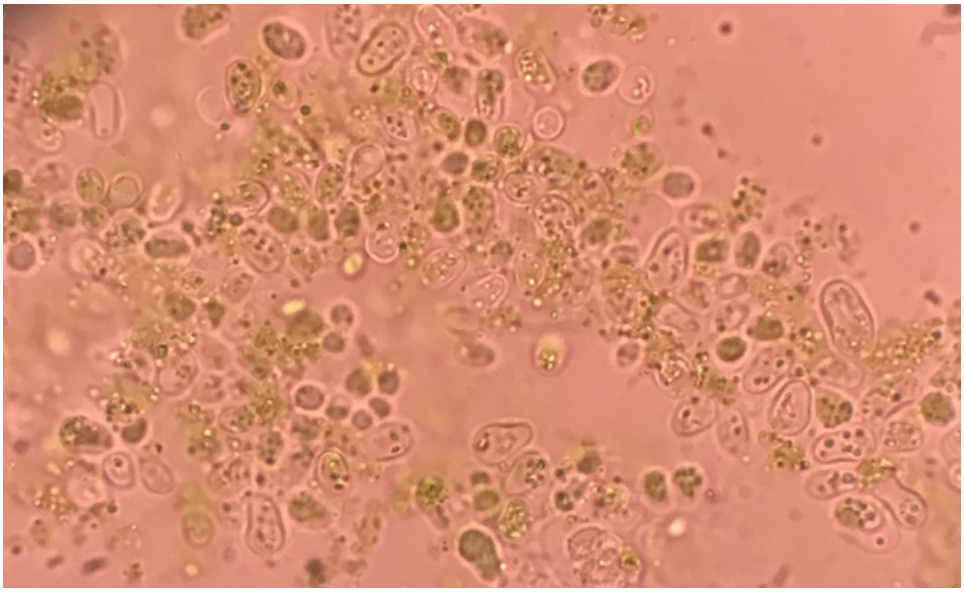


Figure 4.5 *Chlorella minutissima* at logarithmic phase

Table 4.1 Velocities of different flow rates in microfluidics

Flow Rate (μL/min)	Cross-Sectional Area (m^2)	**Velocity (m/s)**
1000	0.00000005	0.33
1500		0.5
2000		0.67
2500		0.83
3000		1

Table 4.2 Reynolds number and Dean number calculations

Flow Rate (μL/min)	**Reynolds Number**	**Dean Number**
1000	73.14	0.43
1500	109.71	0.64
2000	146.28	0.85
2500	182.85	1.066
3000	219.42	1.28

emergence of secondary flow patterns, called Dean flows, due to the combination of pressure-driven flow and centrifugal forces [151]. These calculations are provided in Table 4.1 and Table 4.2. Given that the Reynolds numbers are below 300, it can be concluded that the flow in the system remains laminar regardless of the flow rates. Furthermore, the tables indicate that there is a direct correlation between the increase in flow rate and the rise in Reynolds and Dean numbers, Dean velocity, and drag forces [152].

4.1.3.2 AutoCAD Designs and Microfabricated PDMS-based Microfluidic Platforms

2D microchannel structures drawn using the AutoCAD 2018 for separating microalgae and bacteria can be seen in Figure 4.6. From the illustrations, it is evident that the 2D drawings exhibit variations in both the distance between the turns and the number of turns. The geometry of the devices remains consistent with

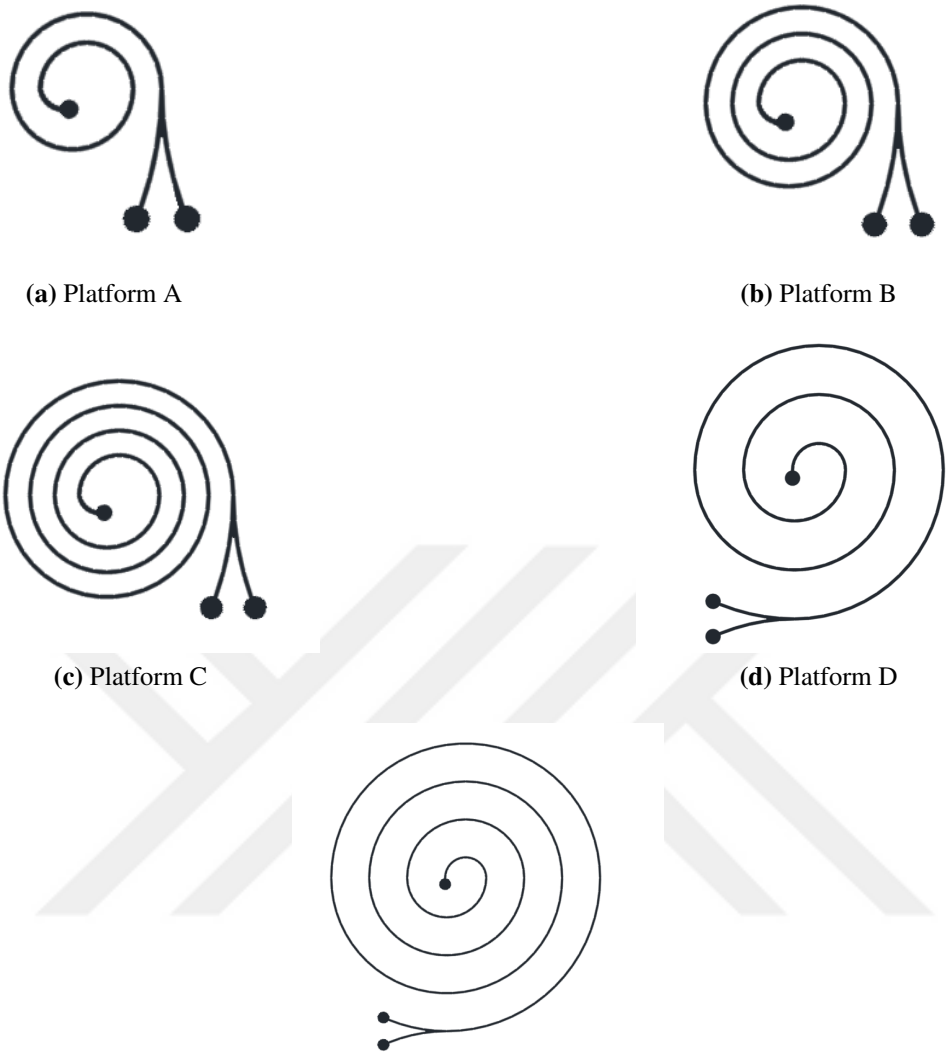
Table 4.3 Dean velocity and drag forces calculations

Flow Rate (μL/min)	**Dean Velocity**	**Drag Force for Microalgae**	**Drag Force for Bacteria**
1000	4,48758E-05	2,02403E-12	5,06007E-13
1500	8,69042E-05	3,91964E-12	9,79909E-13
2000	0,000138896	9,01279E-12	2,2532E-12
2500	0,000199827	1.44046E-13	3.60115E-14
3000	0,00026898	1,21318E-11	3,03295E-12

the microchannel height as 100 μm and a width as 500 μm. The platforms coded as A, B, and C have turn distances of 2 cm and the setting turn numbers of 3, 5, and 7, respectively. On platforms designated as D and E, the spacing between turns is 6 cm. The number of turns on platform D is 5, while on platform E it is 7. The design exploits the forces of inertial lift and viscous drag on particles of different sizes to achieve the separation of microparticles by differential migration.

The spiral microchannels were chosen in the separation system due to their ability in decreasing input energy, enabling the operating to be carried out only by hydrodynamic forces, increasing surface area, enhancing mixing, reducing microalgal clogging, and improving separation performance. The microfluidic system comprises a single input and two output channels. The designs were developed by keeping in mind that that microalgae and bacteria experience centripetal force based on their size disparity and that they will align themselves in accordance with this force within the channel cross-section at different locations.

For laminar flows in both straight and spiral microchannels (Re<2300) particles can be separated due to two different forces: shear gradient-induced and wall-induced buoyancy forces. When particles traverse a straight microchannel, they experience shear stresses, which generate lifting forces perpendicular to the flow direction, in addition to drag forces and normal stresses. Particle separation in the domain of inertial microfluidics is contingent on the attainment of equilibrium between inertial lift and drag forces. The introduction of curves into a straight microchannel induces a secondary flow characterized by centrifugal effects that push particles from the interior wall towards the outer wall. This introduces a third force in spiral microchannels to separate particles depending on their sizes: This is called the secondary-flow drag force called the Dean drag. This secondary flow changes direction near the top and bottom edges of the microchannel, creating two Dean vortices (rotating vortices) inside the spiral microchannel [153, 154].



(a) Platform A

(b) Platform B

(c) Platform C

(d) Platform D

(e) Platform E

Figure 4.6 Microfluidic platform designs

The microalgae and bacteria in spiral microchannels are exposed to the influence of inertial lift forces and dean drag forces during the flow. The parameters of particle size, flow rate, and lift coefficient all have an impact on the inertial lift force's magnitude. As these values rise, the applied force correspondingly increases. Furthermore, the flow rate is a crucial component, as the lift coefficient on particles near the microchannel wall increases with higher Reynolds values. It is worth noting that the flow rate and Reynolds numbers exhibit a direct correlation. This enhances the inertial lift force acting on microalgae particles of large sizes [151, 155].

The interactions between the inertial lift force and dean drag force result in the establishment of a stable location for the particles within the microchannels. Although larger-sized microalgae particles are mostly influenced by the inertial

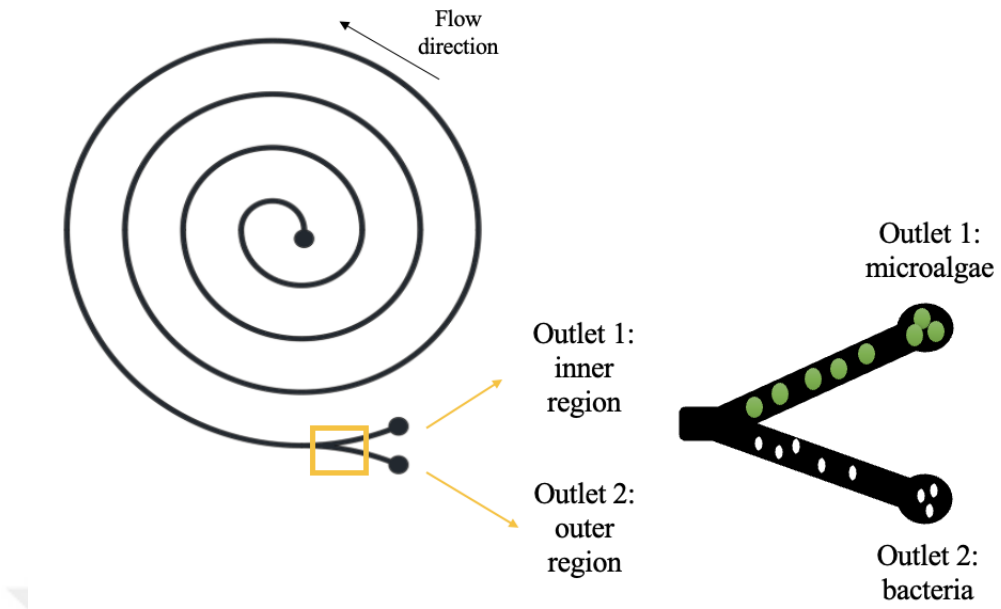


Figure 4.7 Separation of microalgae from bacteria in spiral microchannels

lift forces, smaller-sized bacterial particles are primarily influenced by dean drag forces. Therefore, while microalgae are located in the close region of the microchannel inner wall, bacteria are located in the region of the outer wall of the microchannels [151, 155]. In Figure 4.7, the microchannel on the inside is denoted as channel 1, whereas the microchannel on the outer wall is denoted as channel 2. Theoretically, microalgae are expected to be gathered from outlet channel 1, whereas bacteria are expected to be collected from outlet channel 2.

Microfluidic platforms microfabricated under clean room conditions at Sabancı University SUNUM are shown in Figure A.1. The microchannels were inspected for any blockages or leaks and subsequently cleansed using a solution of 70% ethanol and distilled water in preparation for the experiment.

4.1.4 Separation Performance of Microfluidic Platforms

To effectively separate microalgae and bacteria, the number and distance of turns, as well as the flow rate and channel geometry parameters, should be optimized. Five alternative flow rates were evaluated for each five different microfluidic platform: 1000 μL/min, 1500 μL/min, 2000 μL/min, 2500 μL/min, and 3000 μL/min. An attempt was made to manipulate the flow within the microchannel by adjusting the flow rate. With changes in velocity, the flow's orbital position may incline towards either the inner or outer wall [151].

The separation performance of microfluidic platforms was assessed by calculating

Table 4.4 Separation performance of microfluidic platforms

Microfluidic Platform	Flow Rate (μL/min)	Separation Yield (%)	Separation Purity (%)	Enrichment Factor
A	1000	63.65	89.66	1.09
Microchannel height: 100 μm	1500	62.94	90.02	1.04
Microchannel width: 500 μm	2000	52.80	76.29	1.06
Number of turns: 3	2500	41.18	79.86	1.01
Distance between turns: 2 cm	3000	33.99	66.97	1.03
B	1000	76.59	92.91	1.10
Microchannel height: 100 μm	1500	42.81	81.07	1.30
Microchannel width: 500 μm	2000	60.94	97.23	1.33
Number of turns: 5	2500	58.27	87.43	1.05
Distance between turns: 2 cm	3000	50.51	89.58	0.95
C	1000	34.20	67.53	0.97
Microchannel height: 100 μm	1500	57.99	89.99	1.09
Microchannel width: 500 μm	2000	67.51	89.41	1.05
Number of turns: 7	2500	66.77	90.01	1.06
Distance between turns: 2 cm	3000	60.57	87.06	1.06
D	1000	83.57	94.91	1.05
Microchannel height: 100 μm	1500	82.13	93.49	1.06
Microchannel width: 500 μm	2000	72.52	92.98	1.06
Number of turns: 5	2500	63.98	88.04	1.03
Distance between turns: 6 cm	3000	44.51	85.25	0.98
E	1000	78.09	93.09	1.11
Microchannel height: 100 μm	1500	68.96	86.40	1.16
Microchannel width: 500 μm	2000	72.55	84.65	1.14
Number of turns: 7	2500	69.65	87.64	1.05
Distance between turns: 6 cm	3000	57.74	93.66	1.06

the separation efficiency, separation purity, and enrichment factors using equations 3.7-3.9. The separation performance was evaluated for each individual microfluidic platform at different flow rate and microfluidic chip configurations. Separation performance results are as displayed in Table 4.4.

The separation yield is the proportion of microalgae in the first outlet channel, which is located near the inner wall of the microchannel and is the expected exit location for microalgae, to the total number of cells at the entrance. The separation yield is a crucial factor in assessing the performance of the microfluidic chip platform. It quantifies the rate at which the microalgae is separated from the mixed microorganisms at the entrance and determines whether the microalgae manages to escape to the second outlet channel. The separation yield is displayed in Figure 4.8 for different Reynolds number.

The number of turns was evaluated among microfluidic platforms labeled A, B, and C. The experiments resulted in a separation efficiency of 76.59% when using chip B, which has a circular distance of 2 cm and 5 turns, at a flow rate of 1000 μL/min. There is a minor difference in the separation efficiencies of microfluidic chips A and C, and no separation efficiency over 70% could be obtained. Nevertheless, the separation purity outcomes of microfluidic chip C exceed those of microfluidic

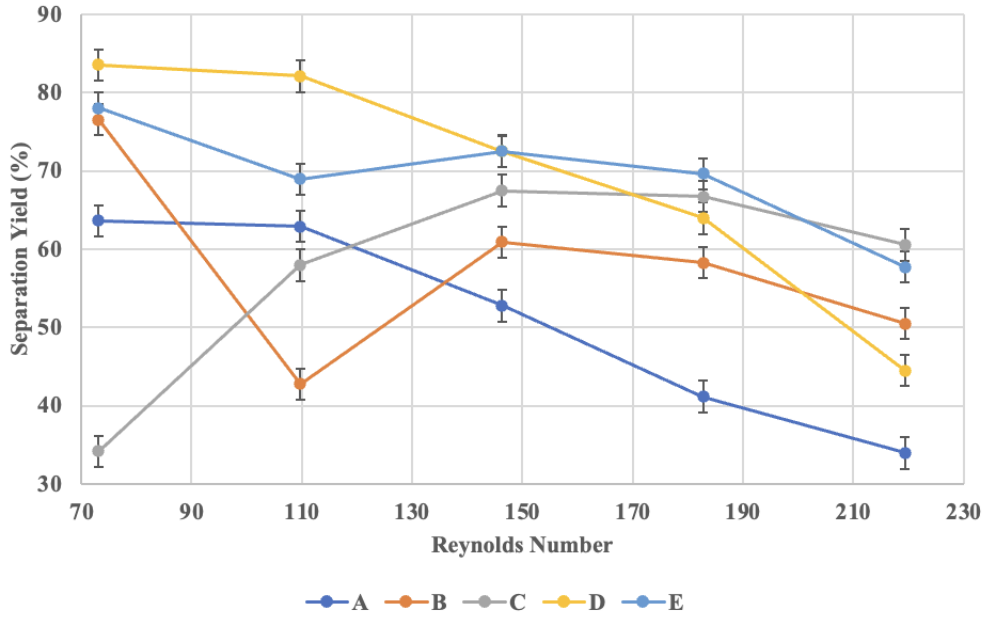


Figure 4.8 Relationship between separation yield as a function of Reynolds number

platform A. In this instance, the microfluidic platform labeled as A has the lowest level of success, characterized by a turn distance of 2 cm and a turn number of 3. This can be attributed to the combination of a small distance between turns and a limited number of turns.

Likewise, a comparison was made between microfluidic platforms D and E based on the number of turns. The highest separation efficiency can be achieved in these studies was 83.57% on chip number D. This was achieved by using a turn distance of 6 cm, a number of turns of 5, and a flow rate of 1000 μL/min. While the separation efficiency results on microfluidic platforms improved when the number of turns was increased from 3 to 5 with a 2 cm distance between turns, the results were negatively impacted when the number of turns was further increased from 5 to 7. Furthermore, increasing of the number of turns from 5 to 7 on microfluidic platforms, with a turn separation distance of 2 cm, had an adverse impact on the results of separation efficiency. Furthermore, the optimal separation efficiency was seen in both the B and D microfluidic platforms when the flow rate was set at 1000 μL/min.

When comparing B and D coded microfluidic chips, the number of turns remains constant at 5, although the spacing between turns varies. The separation efficiency experienced an approximate 7% rise when the inter-turn distance was raised from 2 cm to 6 cm. Similarly, when comparing C and E coded microfluidic platforms, the number of turns remains constant at 7, although the distance between turns changes. The separation efficiency experienced an approximate 2% rise when the inter-turn

distance was raised from 2 cm to 6 cm.

Separation purity refers to the proportion of microalgae in outlet channel number 1, where we aim for the microalgae to be released, compared to the total number of cells in the same channel. It indicates the percentage of purity of the microalgae culture in that specific channel. The relationship of separation purity with Reynolds number is given in Figure 4.9.

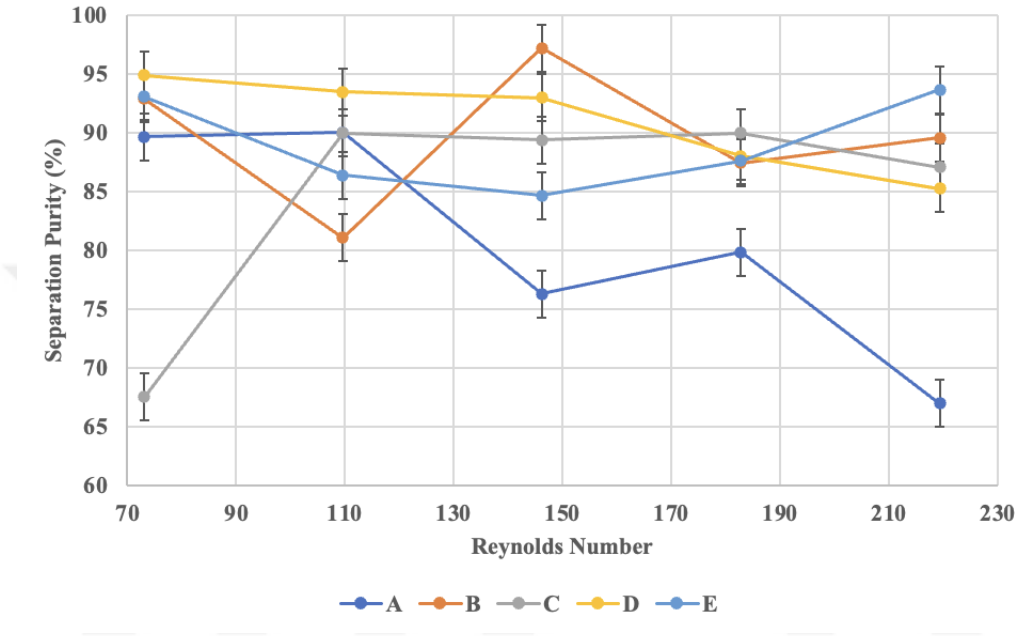


Figure 4.9 Relationship between separation purity and Reynolds number

The number of turns was evaluated among microfluidic platforms labeled A, B, and C. The experiments showed a separation purity of 97.23% when using chip B, which has a circular distance of 2 cm and 5 turns, at a flow rate of 2000 μL/min. Also, The number of turns was evaluated among microfluidic platforms labeled D and E. The experiments showed a separation efficiency of 94.91% when using chip D, which has a circular distance of 6 cm and 5 turns, at a flow rate of 1000 μL/min. Studies indicate that a distance of 6 cm between turns in microfluidic platforms typically results in a separation purity of 85% or higher, leading to the acquisition of a pure culture. Within microfluidic platforms, when the inter-turn distance is 2 cm, the outcomes of separation purity show some difference. There is a noticeable decrease in separation purity when the platform code A is operated at high speeds with 3 turns, and when the platform code C is operated at low speeds with 7 turns.

Similarly, a comparison was made between microfluidic platforms D and E based on the number of turns. The highest separation purity achieved in these studies was 94.91% on chip number D. This was achieved by using a turn distance of 6 cm, a number of turns of 5, and a flow rate of 1000 μL/min. While the separation

efficiency results on microfluidic platforms improved when the number of turns was increased from 3 to 5 with a 2 cm distance between turns, the results are negatively impacted when the number of turns was further increased from 5 to 7.

When comparing B and D-coded microfluidic chips, the number of turns remains constant at 5, although the spacing between turns varies. The separation purity experiences an approximate 2% rise when the inter-turn distance was decreased from 6 cm to 2 cm. Conversely, when comparing C and E-coded microfluidic chip platforms, the number of turns remains constant at 7, although the distance between turns changes. The separation purity experienced an approximate 3.5% rise when the inter-turn distance was raised from 2 cm to 6 cm.

The enrichment factor is calculated by dividing the separation purity ratio by the sum of the number of microalgae in the intake and the total number of cells in the inlet. This ratio provides insight into the degree to which microalgae detach from the initial mixed culture and enhance it. The relationship of enrichment factor with Reynolds number is given in Figure 4.10.

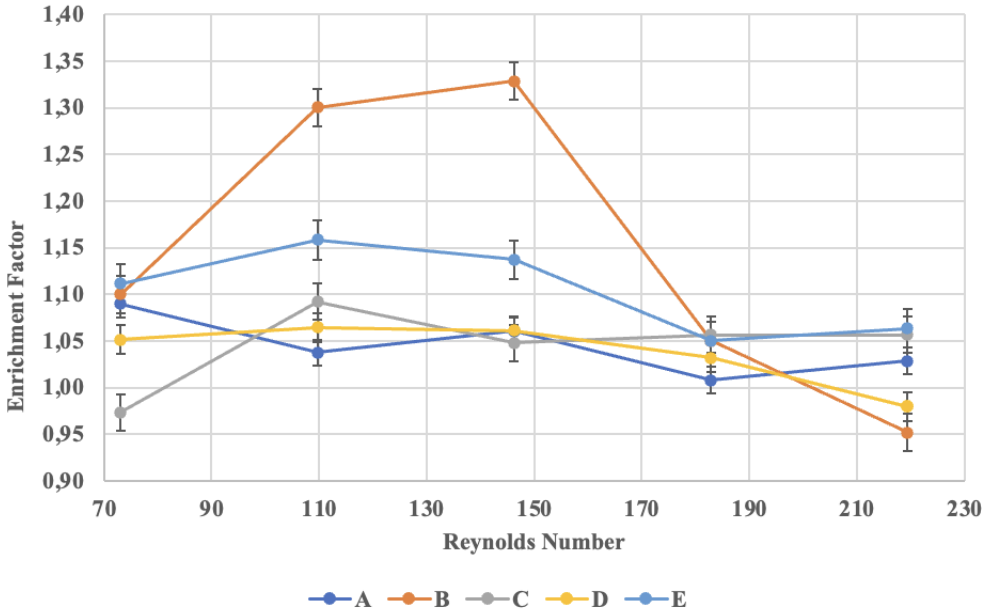


Figure 4.10 Relationship between enrichment factor and Reynolds number

The enrichment factor typically exceeds 1. However, on microfluidic platforms authorized as B and D, the number of turns is 5, and the corresponding values are below 1, specifically 0.95 and 0.98, respectively. The B-coded microfluidic platform achieved the highest enrichment factor of 1.33 and 1.30 at speeds of 2000 μL/min and 1500 μL/min, respectively. Similarly, the E-coded microfluidic platform achieved an enrichment factor of 1.16 and 1.14 at speeds of 2000 μL/min and 1500 μL/min, respectively. For all other velocities and geometries, the enrichment

factor values were determined to be similar to each other, with an average value of 1. The thesis experiments revealed that, apart from the significance of effectively separating microalgae from bacteria and attaining optimal separation yield and purity, it is equally crucial to concentrate the microalgae in the same outlet channel. If microalgae cannot be efficiently gathered in the outlet channel linked to the inner wall and microalgae are detected in the outlet channels connected to the outer wall, it suggests that there is a depletion of microalgae cells.

The evaluation of separation yield, separation purity, and enrichment factor was conducted using different microfluidic platforms. It appeared that the A-coded microfluidic platform had the lowest percentage of success among the usable devices. While the purity and efficacy were comparable at 1000 μL/min and 1500 μL/min flow rates, with the former reaching 90%, the other speed was unable to surpass 65%.

In general, efficiency, purity, and enrichment factor diminish as the Reynolds value rises. The minimum number of turns and the distance between turns in the geometry of the microfluidic platform denoted A are believed to be responsible for this circumstance. As a consequence of increasing the number of turns to 5 on the B-coded microfluidic chip, the separation performance outcomes improved at all velocities with the exception of 1500 μL/min. Furthermore, this chip demonstrated the highest separation purity and enrichment factor; however, it operates at a relatively low efficiency. Upon examination of the Reynolds-related graphs, the outcomes pertaining to the code B platform exhibit a lack of consistency, rendering any assessment of the velocity unfeasible. With the exception of all other microfluidic platforms, the separation performance results of the C-coded chip exhibited a decline as the number of turns increased to seven. Conversely, an enhancement in the results was detected as the Reynolds number increased.

A general enhancement in separation efficiency and separation purity outcomes was observed as the distance between turns increased. It appeared that the D-coded microfluidic platform was the most effective of the working systems. Furthermore, upon comparing D-coded and E-coded microfluidic chips, it appears that the 5-turn D microfluidic chip exhibits superior performance in terms of purity and efficiency. However, in terms of enrichment factor, the E-coded microfluidic chip demonstrates superiority. Upon examination of the data associated with the Reynolds value, the E-coded microfluidic platform yielded consistent results, with the exception of the separation purity and D-coded results. It was observed that as the flow rate increased, the separation performance results tended to diminish.

The findings unequivocally indicate that the optimal flow rate varies among the microfluidic platforms. Because alterations in the microfluidic geometry, such as modifications in the distance between turns, result in variations in the radius of curvature and residence duration of particles within the microchannel, thereby influencing the Dean number, Dean speed, and drag forces, are also possible. The particles' distance traveled and the amount of time they spend within the microchannel will both increase as the number of turns increases. Similarly, alterations in the flow rate will result in corresponding modifications to the Reynolds number, Dean number, Dean speed, and drag forces. Nevertheless, when the optimal flow rate is surpassed, the particles' residence time in the microchannel will diminish, potentially impeding the attainment of adequate residence time for separation processes that are dependent on particle size. Moreover, as Reynolds values increase, flow patterns may be disrupted, resulting in secondary flow disruption and diminished separation performance. Moreover, as Reynolds values increase, the trajectories of the cells may undergo alterations that cause them to diverge from the channel path [153, 156]. Consequently, determining the optimal microchannel configuration and flow rate for this configuration is critical. In Syed et al.'s experiment on microalgae separation using a spiral microfluidic chip, it was noted that the concentration of particles and the efficiency of the process varied with the size of the particles and the flow rate [90]. Furthermore, it was observed that the concentration of particles decreased as the Reynolds number increased, particularly in the case of small-sized cells. Nevertheless, it has been shown that efficiency tends to improve within the range of speeds from 500 to 1000 μL/min. Similar results are seen in the study conducted by Mihandoust et al. [106]. In the spiral microfluidic research conducted to separate two different algae of different sizes, it was observed that the lift coefficient decreased as the Reynolds value exceeded a certain threshold, and this reduced the focusing of especially small-sized particles.

The alteration of the number of turn an distance between them has an impact on the characteristics and potency of secondary flows, encompassing the development of Dean eddies. Upon examination of Table 4.4, it is determined that the D microfluidic platform, comprising five turns spaced 6 cm apart, operates optimally at a velocity of 1000 μL/min for the purpose of segregating microalgae from bacteria. However, it is also important to consider the high purity and enrichment factor outcomes of the B microfluidic platform, which consists of five turns separated by 6 cm. It is noteworthy that microchannels featuring five turns enhance the concentration of both sizable and microorganisms contained within the channel. The trajectories of microalgae and bacterial cells within the channel are influenced by the number of turns and the distance between them [108, 154].

Table 4.5 Separation performance of antibiotic-treatment method in microalgae cultures

Treatment with Antibiotics		
	5 days	15 days
Separation Efficiency (%)	27	99.9
Purity of Culture (%)	97	99.9

Several parameters influence the outcomes of the investigation across the entire experimental set. The potential for variation in separation performance results exists when conducting repeated sets of experiments due to the fact that the growth phase of microalgae influences their size distribution. Additionally, microalgae are typically collapsing microorganisms. At a certain point, microalgae in the sterile syringe containing the inlet flow may begin to precipitate and accumulate during the microchannel flow, thereby influencing the experimental outcome. Moreover, as the investigation progresses and the syringe is refilled after the sample in it is depleted, the concentrations of microorganisms in the syringe may fluctuate. Varied concentration profiles have the potential to induce variations in separation efficiency, purity, and enrichment factor. In the study carried out by Godino et al. in a flat microchannel, 1 and 20 micron beads were used to separate bacteria and microalgae. In this study, it was observed that the separation efficiency and separation purity decreased as the initial concentration of large particles increased [10]. Microalgae and bacterial cells used in high concentrations for ease of analysis in this experiment may have reduced the separation performance [155]. Moreover, the potential for bacterial proliferation in the samples accumulated for counting in eppendorf tubes following the separation experiment, as well as the sensitivity and accuracy of the colony counting methods selected for bacterial counting, may also have an impact on the experimental outcome. Considering that the experiments were carried out at Yıldız Technical University and Sabancı University, it is possible that experimental parameters, including temperature and pressure, influenced the outcomes as well [153].

4.1.5 Separation Performance of Antibiotic-Treatment Method

The identical combination of microalgae and bacteria that was initially synthesized for separation in microfluidic devices was also prepared for eliminate bacteria using antibiotics, yielding the findings presented in Table 4.5. The table indicates that a separation efficiency and separation purity of about 100% were attained within a span of 10 days after 5 days cultivation with antibiotics.

Despite the apparent success indicated in the table, the process of separating with antibiotics carries numerous drawbacks. The primary drawbacks include the utilization of chemicals, extended cultivation periods, the production of waste, and the subsequent requirement for a distinct procedure to removing the culture from antibiotics.

Furthermore, considering that the primary objective of the thesis is to isolate microalgae from samples originating from Antarctica, the application of antibiotics on samples obtained from the polar region also presents a significant uncertainty. The samples from the poles contain highly valuable and distinct types of microorganisms. To ensure optimal results, it is crucial to utilize microfluidic devices that allow for the collection of various bacteria from separate outlets and enable microalgal enrichment. This approach is preferable to the traditional way of isolating and separating germs through antibiotic-induced death. Furthermore, it is worth noting that even when employing the isolation technique with antibiotics, it is possible to encounter antibiotic resistance in species obtained from natural sources.

Moreover, during the antibiotic experiments carried out on polar samples at Yıldız Technical University Algal Bioprocess and Biotechnology Laboratory, it was noted that the application of antibiotics to certain microalgae species resulted in a color change from green to white in the culture. This change, accompanied by the death of both the microalgae and the bacteria, was particularly evident in the isolation of polar microalgae. Also, antibiotic disks were found to cause a reduction in the growth kinetics of certain species. These findings demonstrate the antibiotic resistance of certain microalgae species. Thus, it appears that the employment of antibiotics as an isolation approach is not universally applicable to all species of microalgae.

4.1.6 Comparing Biochemical Contents and Growth Kinetics of Microalgae Cultures After Novel and Traditional Separation Methods

Biochemical contents were examined of

- Culture was subjected to a 5-day antibiotic treatment,
- Culture obtained serial dilution and recultivation with antibiotics for an additional 10 days after 5-day antibiotic treatment,
- Culture obtained after the separation process with a D-coded microfluidic chip with a geometry of 5 turns and a 6 cm inter-turn distance at a flow rate of 1000 μL/min and 10-day recultivation and,

Table 4.6 Comparing biochemical contents of microalgae cultures

Biochemical Contents	Untreated Microalgae Culture	Cultivation After Microfluidics	Treatment with Antibiotics	
	10 days	10 days	5 days	15 days
Carbohydrate Content (µg/mL)	200.5	400	122.5	349.5
Protein Content (µg/mL)	98.6	142.86	6.14	5.9
Chlorophyll Content (µg/mL)	2.15	3	0.9	0.28
Carotene Content(µg/mL)	0.9	1.11	0.3	0.108

- 10- day pure microalgae culture without any treatment

in Table 4.6.

The microalgae culture that was recultured after being separated from the microfluidic platform had the highest levels of carbohydrates, proteins, and pigments among all cultures. These findings are expected because microfluidic systems can serve as pretreatment in microalgal bioprocesses [157, 158]. For instance, microfluidic chips stimulate the formation of astaxanthin by exerting mechanical pressure on *H. pluvialis* cells with a specific channel structure [127].

As the period of antibiotic treatment increased, a reduction in protein and pigment levels was noted in the treated cultures. The microalgae culture treated with antibiotics for a duration of 15 days exhibited the least amount of protein and pigment content. The reason for this is that antibiotics have an impact on the growth of microalgae, block the creation of chloroplasts, as well as the production of chlorophyll-a, beta-carotene, and several enzymes (proteins) [159, 160]. The increase in carbohydrate content of the culture is to be expected. The microalgae were cultured for an initial duration of 5 days, and the culture was then extended for an additional 10 days, resulting in a total culture period of 15 days. Protein and pigment synthesis were suppressed, redirecting their metabolic processes towards the production of carbohydrates, which is the main metabolic product. Nevertheless, it was unable to exceed the quantity of carbohydrates acquired through the recultivation of microalgae that were isolated from the microfluidic platform after a 15-day period of cultivation. Similarly, Leng et al. stated that biochemical activities and biomass growth of microalgae such as photosynthesis,

antioxidant system activities and carotenoid biosynthesis may be affected by antibiotics [159].

Furthermore, the growth kinetics of the cultures were also analyzed in addition to these findings. After a 10-day culture period, the microalgae that were cultivated using the microfluidic chip exhibited the most favorable growth as shown in Figure 4.11. After a period of 10 days, the absorbance value at a wavelength of 680 nm for the cultures that were separated by the chip reached approximately 1, whereas the absorbance value for the pure culture was around 0.6. The initial absorbance values of both cultures were similar. The calculations revealed that the growth rate of the pure culture was determined to be 0.36 day^{-1}, the growth rate of the culture treated with antibiotics was 0.3 day^{-1}, and the growth rate of the culture separated by chip was 0.49 day^{-1}. Additionally, the R^2 values for all three cases were found to be 1. These findings demonstrate that the application of shear stress in microchannels promotes cell development and enhances their biochemical composition without inducing any cellular harm. Wu et al. performed the separation of *H. pluvialis* and *C. vulgaris* using a microfluidic chip. They demonstrated that *C. vulgaris* exhibited superior growth after the separation compared to pure culture, like our results [155].

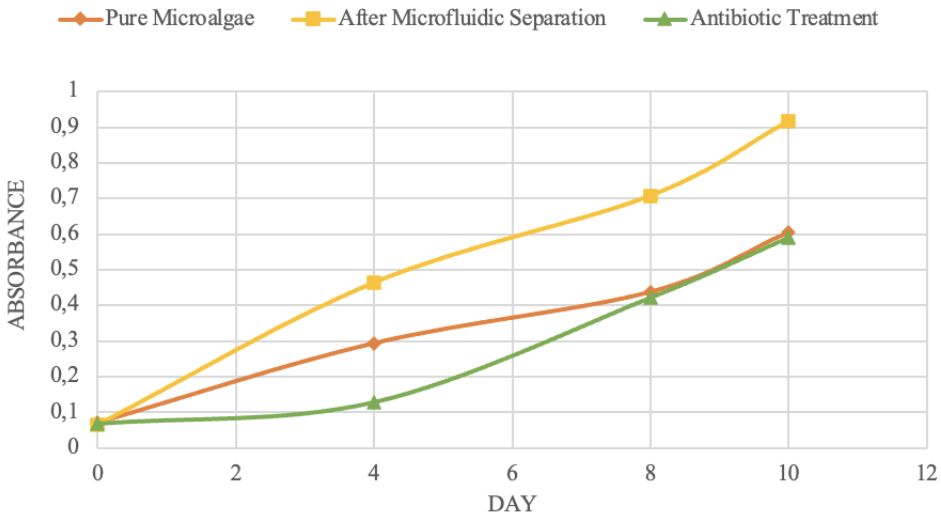


Figure 4.11 Growth kinetics of three different microalgae culture

4.2 Conclusion and Future Perspectives

Microfluidic devices were effectively utilized to separate and enrich microalgae based on their different sizes and inertial forces. Following the separation procedure, the microalgae were then cultivated again. Upon investigating the impact of microfluidic systems on the growth and biochemical composition of microalgae, it was observed that the system yielded favorable outcomes.

- Microfluidic systems have been developed to separate and enrich microalgae from bacteria via spiral microchannels.
- The impact of channel geometry on separation performance was investigated by altering the parameters of the number of turns and distance between turns in spiral microchannels, which were designed using AUTOCAD.
- Among the spiral microchannels with 3, 5, and 7 turns, the most optimal one is the channel with 5 turns. The best separation purity and enrichment factor were achieved with a distance between the turns of 2 cm, while the highest separation efficiency was obtained with a distance of 6 cm.
- The most consistent results were obtained from the microfluidic platform configuration where the number of turns was 5 and the distance between turns was 6 cm.
- The effect of flow rate on separation performance was examined by testing flow rates between 1000 μL/min and 3000 μL/min. By increasing the flow rate in the microfluidic platform with 7 turns and a 2 cm distance between them, the separation performance could be improved. However, in all other microfluidic platforms, the Reynolds value and separation performance were generally found to be inversely proportional.
- The best flow rate results were achieved at 1000 μL/min and 1500 μL/min in the microchannel geometry with a channel width of 500 μm, channel height of 100 μm, inlet channel inner diameter of 3 cm, and a number of turns of 5.
- The interaction between particles of varying sizes and the fluid flow pattern in the spiral microchannel results in the arrangement and separation of particles based on their size.
- Bacteria were eliminated from the microalgae culture through the use of antibiotic disks, resulting in their complete removal after a 15-day treatment period. Nevertheless, it is evident that the administration of antibiotics adversely impacts the growth of microalgae and their biochemical composition.
- Following the size-based separation process using microfluidic technology, there was an obvious enhancement in the growth and biochemical composition of the cultivated microalgae.

The microfluidic device, which was specifically designed and optimized in terms

of microchannel geometry and flow rate, was prove to be effective in sorting and concentrating microalgae in samples obtained from polar regions.

Separation performance results can be improved by adding an external power source to the designed system or by creating a cascade microfluidic system with an additional spiral or serpentine channel both approaches will introduce additional pressure losses and input power.

For the purpose of simplified cell counting analysis, we utilized huge amounts of microalgae and bacterial cells while keeping the cell number constant in this experiment. Nevertheless, it is expected that more purity can be attained by cultivating cultures with significantly reduced densities of microalgae cells or by performing studies with polar samples.

These results fill in some gaps in our knowledge about how the number of turns and the distance between them in spiral microchannels affect the ability to separate microorganisms based on their sizes, growth, and the biochemical content of microalgae.

The optimized PDMS-based microfluidic platform has the potential for the used in the applications future polar science expeditions. Similarly, it can be used not only for the isolation of microalgae from polar samples but also from samples obtained from nature, such as seas, lakes, oceans, etc. Apart from microalgae isolation, microfluidic chip platforms can be used to obtain pure microalgae culture and to remove impurities from contaminated cultures. Finally, the optimized microfluidic platform has a high potential for the use in the applications of the growth of microalgae cultures and increasing their biochemical content.

REFERENCES

[1] J. L. Harwood, I. A. Guschina, "The versatility of algae and their lipid metabolism," *Biochimie*, vol. 91, no. 6, pp. 679–684, 2009.

[2] A. Lehmuskero, M. S. Chauton, T. Boström, "Light and photosynthetic microalgae: A review of cellular-and molecular-scale optical processes," *Progress in oceanography*, vol. 168, pp. 43–56, 2018.

[3] B. R. Lyon, T. Mock, "Polar microalgae: New approaches towards understanding adaptations to an extreme and changing environment," *Biology*, vol. 3, no. 1, pp. 56–80, 2014.

[4] A.-G. Niculescu, C. Chircov, A. C. Bircă, A. M. Grumezescu, "Fabrication and applications of microfluidic devices: A review," *International Journal of Molecular Sciences*, vol. 22, no. 4, p. 2011, 2021.

[5] Q. Zhong, H. Ding, B. Gao, Z. He, Z. Gu, "Advances of microfluidics in biomedical engineering," *Advanced materials technologies*, vol. 4, no. 6, p. 1 800 663, 2019.

[6] B. Karacaoğlu, B. İnan, D. B. Özçimen, "Microfluidic systems as a novel approach for microalgal bioprocess," *Biochemical Engineering Journal*, vol. 197, p. 108 959, 2023.

[7] B. Ozdalgic, M. Ustun, S. R. Dabbagh, B. Z. Haznedaroglu, A. Kiraz, S. Tasoglu, "Microfluidics for microalgal biotechnology," *Biotechnology and Bioengineering*, vol. 118, no. 4, pp. 1716–1734, 2021.

[8] S.-M. Paik, S.-J. Sim, N. L. Jeon, "Microfluidic perfusion bioreactor for optimization of microalgal lipid productivity," *Bioresource technology*, vol. 233, pp. 433–437, 2017.

[9] H. S. Kwak, J. Y. H. Kim, S. J. Sim, "A microreactor system for cultivation of haematococcus pluvialis and astaxanthin production," *Journal of nanoscience and nanotechnology*, vol. 15, no. 2, pp. 1618–1623, 2015.

[10] N. Godino, F. Jorde, D. Lawlor, M. Jaeger, C. Duschl, "Purification of microalgae from bacterial contamination using a disposable inertia-based microfluidic device," *Journal of Micromechanics and Microengineering*, vol. 25, no. 8, p. 084 002, 2015.

[11] X. Cheng, Z. Qi, T. Burdyny, T. Kong, D. Sinton, "Low pressure supercritical co2 extraction of astaxanthin from haematococcus pluvialis demonstrated on a microfluidic chip," *Bioresource technology*, vol. 250, pp. 481–485, 2018.

[12] Y. Yang *et al.*, "A microfluidic system for viability determination of microalgae upon disinfectant treatment under continuous flow," *Science of The Total Environment*, vol. 816, p. 151 615, 2022.

[13] A. Gosset *et al.*, "Xurography-based microfluidic algal biosensor and dedicated portable measurement station for online monitoring of urban polluted samples," *Biosensors and Bioelectronics*, vol. 117, pp. 669–677, 2018.

[14] M. B. Akolpoglu, N. O. Dogan, U. Bozuyuk, H. Ceylan, S. Kizilel, M. Sitti, "High-yield production of biohybrid microalgae for on-demand cargo delivery," *Advanced Science*, vol. 7, no. 16, p. 2 001 256, 2020.

[15] M. Romanello *et al.*, "The 2022 report of the lancet countdown on health and climate change: Health at the mercy of fossil fuels," *The Lancet*, vol. 400, no. 10363, pp. 1619–1654, 2022.

[16] J. C. Xavier *et al.*, "A review on the biodiversity, distribution and trophic role of cephalopods in the arctic and antarctic marine ecosystems under a changing ocean," *Marine biology*, vol. 165, pp. 1–26, 2018.

[17] X. Rodó, A. San-José, K. Kirchgatter, L. López, "Changing climate and the covid-19 pandemic: More than just heads or tails," *Nature Medicine*, vol. 27, no. 4, pp. 576–579, 2021.

[18] A. Gray *et al.*, "Remote sensing reveals antarctic green snow algae as important terrestrial carbon sink," *Nature Communications*, vol. 11, no. 1, p. 2527, 2020.

[19] S. Ahmad, A. Pandey, V. V. Pathak, V. V. Tyagi, R. Kothari, "Phycoremediation: Algae as eco-friendly tools for the removal of heavy metals from wastewaters," *Bioremediation of Industrial Waste for Environmental Safety: Volume II: Biological Agents and Methods for Industrial Waste Management*, pp. 53–76, 2020.

[20] S. Khan, P. Fu, "Biotechnological perspectives on algae: A viable option for next generation biofuels," *Current opinion in biotechnology*, vol. 62, pp. 146–152, 2020.

[21] E. Daneshvar, R. J. Wicker, P.-L. Show, A. Bhatnagar, "Biologically-mediated carbon capture and utilization by microalgae towards sustainable co2 biofixation and biomass valorization–a review," *Chemical Engineering Journal*, vol. 427, p. 130 884, 2022.

[22] M. N. Metsoviti, G. Papapolymerou, I. T. Karapanagiotidis, N. Katsoulas, "Comparison of growth rate and nutrient content of five microalgae species cultivated in greenhouses," *Plants*, vol. 8, no. 8, p. 279, 2019.

[23] A. Olabi *et al.*, "Role of microalgae in achieving sustainable development goals and circular economy," *Science of The Total Environment*, vol. 854, p. 158 689, 2023.

[24] H. Peng, L. E. de-Bashan, B. T. Higgins, "Comparison of algae growth and symbiotic mechanisms in the presence of plant growth promoting bacteria and non-plant growth promoting bacteria," *Algal Research*, vol. 53, p. 102 156, 2021.

[25] K. Thiyagarasaiyar, B.-H. Goh, Y.-J. Jeon, Y.-Y. Yow, "Algae metabolites in cosmeceutical: An overview of current applications and challenges," *Marine drugs*, vol. 18, no. 6, p. 323, 2020.

[26] Y. Xie *et al.*, "Advancement of renewable energy technologies via artificial and microalgae photosynthesis," *Bioresource Technology*, vol. 363, p. 127 830, 2022.

[27] R. Prasad *et al.*, "Role of microalgae in global co2 sequestration: Physiological mechanism, recent development, challenges, and future prospective," *Sustainability*, vol. 13, no. 23, p. 13 061, 2021.

[28] R. T. Lindberg, S. Collins, "Quality–quantity trade-offs drive functional trait evolution in a model microalgal 'climate change winner'," *Ecology letters*, vol. 23, no. 5, pp. 780–790, 2020.

[29] A. Hopes, D. N. Thomas, T. Mock, "Polar microalgae: Functional genomics, physiology, and the environment," *Psychrophiles: From Biodiversity to Biotechnology*, pp. 305–344, 2017.

[30] R. J. Duncan, K. Petrou, "Biomolecular composition of sea ice microalgae and its influence on marine biogeochemical cycling and carbon transfer through polar marine food webs," *Geosciences*, vol. 12, no. 1, p. 38, 2022.

[31] T. Maksym, "Arctic and antarctic sea ice change: Contrasts, commonalities, and causes," *Annual Review of Marine Science*, vol. 11, pp. 187–213, 2019.

[32] A. K. DuVivier, M. M. Holland, J. E. Kay, S. Tilmes, A. Gettelman, D. A. Bailey, "Arctic and antarctic sea ice mean state in the community earth system model version 2 and the influence of atmospheric chemistry," *Journal of Geophysical Research: Oceans*, vol. 125, no. 8, e2019JC015934, 2020.

[33] C. Lauritano, C. Rizzo, A. Lo Giudice, M. Saggiomo, "Physiological and molecular responses to main environmental stressors of microalgae and bacteria in polar marine environments," *Microorganisms*, vol. 8, no. 12, p. 1957, 2020.

[34] S. Cao *et al.*, "Structure and function of the arctic and antarctic marine microbiota as revealed by metagenomics," *Microbiome*, vol. 8, pp. 1–12, 2020.

[35] A. D. P. G. Russo, M. S. de Souza, C. R. B. Mendes, B. Jesus, V. M. Tavano, C. A. E. Garcia, "Photophysiological effects of fe concentration gradients on diatom-dominated phytoplankton assemblages in the antarctic peninsula region," *Journal of Experimental Marine Biology and Ecology*, vol. 466, pp. 49–58, 2015.

[36] S. Venkatachalam, G. F. Matcher, T. Lamont, M. van den Berg, I. J. Ansorge, R. A. Dorrington, "Influence of oceanographic variability on near-shore microbial communities of the sub-antarctic prince edward islands," *Limnology and Oceanography*, vol. 64, no. 1, pp. 258–271, 2019.

[37] J. Matsuo, S. Nakamura, T. Okubo, M. Fukui, H. Yamaguchi, "Long-term survival of naegleria polaris from antarctica after 10 years of storage at 4° c," *Parasitology research*, vol. 117, pp. 937–941, 2018.

[38] M.-L. Teoh, W.-L. Chu, H. Marchant, S.-M. Phang, "Influence of culture temperature on the growth, biochemical composition and fatty acid profiles of six antarctic microalgae," *Journal of Applied Phycology*, vol. 16, pp. 421–430, 2004.

[39] A. Ugur, O. S. YILMAZ, F. B. SANLI, D. OZCIMEN, "A new method for fully automated detection of algae blooms in antarctica using sentinel-2 satellite images," *Advances in Space Research*, 2023.

[40] D. F. Soto, R. Fuentes, P. Huovinen, I. Gómez, "Microbial composition and photosynthesis in antarctic snow algae communities: Integrating metabarcoding and pulse amplitude modulation fluorometry," *Algal Research*, vol. 45, p. 101 738, 2020.

[41] N. A. Yusof, N. H. F. Hashim, I. Bharudin, "Cold adaptation strategies and the potential of psychrophilic enzymes from the antarctic yeast, glaciozyma antarctica pi12," *Journal of Fungi*, vol. 7, no. 7, p. 528, 2021.

[42] V. V. Doytchinov, S. G. Dimov, "Microbial community composition of the antarctic ecosystems: Review of the bacteria, fungi, and archaea identified through an ngs-based metagenomics approach," *Life*, vol. 12, no. 6, p. 916, 2022.

[43] T. R. e. Silva *et al.*, "Pigments from antarctic bacteria and their biotechnological applications," *Critical Reviews in Biotechnology*, vol. 41, no. 6, pp. 809–826, 2021.

[44] N. D. Zamree *et al.*, "The utilisation of antarctic microalgae isolated from paradise bay (antarctic peninsula) in the bioremediation of diesel," *Plants*, vol. 12, no. 13, p. 2536, 2023.

[45] Z. S. Lim *et al.*, "Harnessing diesel-degrading potential of an antarctic microalga from greenwich island and its physiological adaptation," *Biology*, vol. 12, no. 8, p. 1142, 2023.

[46] W. Luo *et al.*, "Molecular diversity of the microbial community in coloured snow from the fildes peninsula (king george island, maritime antarctica)," *Polar Biology*, vol. 43, pp. 1391–1405, 2020.

[47] M. P. Davey *et al.*, "Snow algae communities in antarctica: Metabolic and taxonomic composition," *New Phytologist*, vol. 222, no. 3, pp. 1242–1255, 2019.

[48] M.-L. Teoh, W.-L. Chu, S.-M. Phang, "Effect of temperature change on physiology and biochemistry of algae: A review," *Malaysian Journal of Science*, vol. 29, no. 2, pp. 82–97, 2010.

[49] B. İnan *et al.*, "Interactive effects of cold and temperate conditions on growth and biochemical content of antarctic microalga chlorella variabilis ytu. antarctic. 001," *Journal of Applied Phycology*, vol. 35, no. 2, pp. 625–637, 2023.

[50] M. Cvetkovska, G. Vakulenko, D. R. Smith, X. Zhang, N. P. Hüner, "Temperature stress in psychrophilic green microalgae: Minireview," *Physiologia Plantarum*, vol. 174, no. 6, e13811, 2022.

[51] D. Morales-Sánchez, P. S. Schulze, V. Kiron, R. H. Wijffels, "Temperature-dependent lipid accumulation in the polar marine microalga chlamydomonas malina rcc2488," *Frontiers in Plant Science*, vol. 11, p. 619 064, 2020.

[52] M.-L. Teoh, S.-M. Phang, W.-L. Chu, "Response of antarctic, temperate, and tropical microalgae to temperature stress," *Journal of Applied Phycology*, vol. 25, pp. 285–297, 2013.

[53] P. S. Schulze, C. J. Hulatt, D. Morales-Sánchez, R. H. Wijffels, V. Kiron, "Fatty acids and proteins from marine cold adapted microalgae for biotechnology," *Algal Research*, vol. 42, p. 101 604, 2019.

[54] S. Anuwar, M.-L. Teoh, W.-H. Yap, F.-L. NG, S.-M. PHANG, "Effects of elevated temperatures on growth and photosynthetic performance of polar chlorella," *Adv Polar Sci*, vol. 31, no. 2, pp. 124–131, 2020.

[55] K. Cao *et al.*, "The eurythermal adaptivity and temperature tolerance of a newly isolated psychrotolerant arctic chlorella sp.," *Journal of Applied Phycology*, vol. 28, pp. 877–888, 2016.

[56] P. O. de Souza *et al.*, "Bioprospecting of new antarctic seaweed selective antitumor molecules: Chemical characterization and in vitro analysis," *Phytomedicine Plus*, vol. 2, no. 2, p. 100 246, 2022.

[57] B. İnan, B. Mutlu, G. A. Karaca, R. Ç. Koç, D. Özçimen, "Bioprospecting antarctic microalgae as anticancer agent against pc-3 and ags cell lines," *Biochemical Engineering Journal*, vol. 195, p. 108 900, 2023.

[58] V. Ortseifen, M. Viefhues, L. Wobbe, A. Grünberger, "Microfluidics for biotechnology: Bridging gaps to foster microfluidic applications," *Frontiers in Bioengineering and Biotechnology*, vol. 8, p. 589 074, 2020.

[59] C. Tian, Q. Tu, W. Liu, J. Wang, "Recent advances in microfluidic technologies for organ-on-a-chip," *TrAC Trends in Analytical Chemistry*, vol. 117, pp. 146–156, 2019.

[60] S. Battat, D. A. Weitz, G. M. Whitesides, "An outlook on microfluidics: The promise and the challenge," *Lab on a Chip*, vol. 22, no. 3, pp. 530–536, 2022.

[61] H. Esmaeili Khoshmardan, R. Askari Moghadam, "Enhancing capillary force in glass microfluidics devices for bioengineering applications," *Journal of Bioengineering Research*, vol. 1, no. 4, pp. 19–28, 2019.

[62] S. Sarkar, A. F. Nieuwenhuis, S. G. Lemay, "Integrated glass microfluidics with electrochemical nanogap electrodes," *Analytical Chemistry*, vol. 95, no. 9, pp. 4266–4270, 2023.

[63] A. Mekonen, S. Abebe, T. Adali, "Microfluidics devices manufacturing and biomedical applications," *J. Biosens Bioelectron*, vol. 10, p. 1 000 265, 2019.

[64] A. K. Sen, A. Raj, U. Banerjee, S. R. Iqbal, "Soft lithography, molding, and micromachining techniques for polymer micro devices," *Microfluidic Electrophoresis: Methods and Protocols*, pp. 13–54, 2019.

[65] N. Zhang, J. Liu, H. Zhang, N. J. Kent, D. Diamond, M. D. Gilchrist, "3d printing of metallic microstructured mould using selective laser melting for injection moulding of plastic microfluidic devices," *Micromachines*, vol. 10, no. 9, p. 595, 2019.

[66] S. M. Scott, Z. Ali, "Fabrication methods for microfluidic devices: An overview," *Micromachines*, vol. 12, no. 3, p. 319, 2021.

[67] C. Chande *et al.*, "Universal method for fabricating pdms microfluidic device using su8, 3d printing and soft lithography," *Technology*, vol. 8, no. 01n02, pp. 50–57, 2020.

[68] K. Erdem, V. E. Ahmadi, A. Kosar, L. Kuddusi, "Differential sorting of microparticles using spiral microchannels with elliptic configurations," *Micromachines*, vol. 11, no. 4, p. 412, 2020.

[69] D. Pan, Y. Zhang, T. Zhang, B. Li, "Flow regimes of polymeric fluid droplet formation in a co-flowing microfluidic device," *Colloid and Interface Science Communications*, vol. 42, p. 100 392, 2021.

[70] Z. Abdelmalek, A. D'Orazio, A. Karimipour, "The effect of nanoparticle shape and microchannel geometry on fluid flow and heat transfer in a porous microchannel," *Symmetry*, vol. 12, no. 4, p. 591, 2020.

[71] F. Raji, A. Kahani, M. Sahabi, A. Rahbar-kalishami, L. Padrela, "Investigating the effectiveness of the main channel in microfluidic liquid-liquid extraction process," *International Communications in Heat and Mass Transfer*, vol. 147, p. 106 986, 2023.

[72] B. Dash, J. Nanda, S. K. Rout, "The role of microchannel geometry selection on heat transfer enhancement in heat sinks: A review," *Heat Transfer*, vol. 51, no. 2, pp. 1406–1424, 2022.

[73] M. Abdelkarim, N. H. Abd Ellah, M. Elsabahy, M. Abdelgawad, S. A. Abouelmagd, "Microchannel geometry vs flow parameters for controlling nanoprecipitation of polymeric nanoparticles," *Colloids and Surfaces A: Physicochemical and Engineering Aspects*, vol. 611, p. 125 774, 2021.

[74] L.-L. Zhuang *et al.*, "The characteristics and influencing factors of the attached microalgae cultivation: A review," *Renewable and Sustainable Energy Reviews*, vol. 94, pp. 1110–1119, 2018.

[75] D. Öztay, B. İnan, A. T. Koçer, D. Özçimen, "Effect of metallic nanoparticles on microalgal growth and lipid accumulation for biodiesel production," *Brazilian Journal of Chemical Engineering*, vol. 40, no. 1, pp. 103–114, 2023.

[76] E. Lee, M. Jalalizadeh, Q. Zhang, "Growth kinetic models for microalgae cultivation: A review," *Algal research*, vol. 12, pp. 497–512, 2015.

[77] P. Darvehei, P. A. Bahri, N. R. Moheimani, "Model development for the growth of microalgae: A review," *Renewable and Sustainable Energy Reviews*, vol. 97, pp. 233–258, 2018.

[78] P. Benner, L. Meier, A. Pfeffer, K. Krüger, J. E. Oropeza Vargas, D. Weuster-Botz, "Lab-scale photobioreactor systems: Principles, applications, and scalability," *Bioprocess and Biosystems Engineering*, vol. 45, no. 5, pp. 791–813, 2022.

[79] H. S. Kim, T. L. Weiss, H. R. Thapa, T. P. Devarenne, A. Han, "A microfluidic photobioreactor array demonstrating high-throughput screening for microalgal oil production," *Lab on a Chip*, vol. 14, no. 8, pp. 1415–1425, 2014.

[80] C. Dusny, A. Grünberger, C. Probst, W. Wiechert, D. Kohlheyer, A. Schmid, "Technical bias of microcultivation environments on single-cell physiology," *Lab on a Chip*, vol. 15, no. 8, pp. 1822–1834, 2015.

[81] M. G. Saad *et al.*, "High-throughput screening of chlorella vulgaris growth kinetics inside a droplet-based microfluidic device under irradiance and nitrate stress conditions," *Biomolecules*, vol. 9, no. 7, p. 276, 2019.

[82] S. Mishra, Y. Liu, C. Chen, D. Yao, "An easily accessible microfluidic chip for high-throughput microalgae screening for biofuel production. energies 2021, 14, 1817," *Microalgae Cultures*, p. 35, 2021.

[83] C. Westerwalbesloh *et al.*, "A microfluidic photobioreactor for simultaneous observation and cultivation of single microalgal cells or cell aggregates," *PLoS One*, vol. 14, no. 4, e0216093, 2019.

[84] G. Zheng *et al.*, "Microfluidic chemostatic bioreactor for high-throughput screening and sustainable co-harvesting of biomass and biodiesel in microalgae," *Bioactive Materials*, vol. 25, pp. 629–639, 2023.

[85] H. S. Kwak, J. Y. H. Kim, H. M. Woo, E. Jin, B. K. Min, S. J. Sim, "Synergistic effect of multiple stress conditions for improving microalgal lipid production," *Algal Research*, vol. 19, pp. 215–224, 2016.

[86] C. Castaldello, E. Sforza, E. Cimetta, T. Morosinotto, F. Bezzo, "Microfluidic platform for microalgae cultivation under non-limiting co2 conditions," *Industrial & Engineering Chemistry Research*, vol. 58, no. 39, pp. 18 036–18 045, 2019.

[87] H. Abdulla Yusuf, S. Z. Hossain, A. A. Khamis, H. T. Radhi, A. S. Jaafar, P. R. Fielden, "A hybrid microfluidic differential carbonator approach for enhancing microalgae growth: Inline monitoring through optical imaging," *Arabian Journal for Science and Engineering*, vol. 46, pp. 6765–6774, 2021.

[88] A. Abdelfattah *et al.*, "Microalgae-based wastewater treatment: Mechanisms, challenges, recent advances, and future prospects," *Environmental Science and Ecotechnology*, vol. 13, p. 100 205, 2023.

[89] A. Mehta, "Downstream processing for biopharmaceuticals recovery," *Pharmaceuticals from Microbes: The Bioengineering Perspective*, pp. 163–190, 2019.

[90] M. S. Syed *et al.*, "Selective separation of microalgae cells using inertial microfluidics," *Bioresource technology*, vol. 252, pp. 91–99, 2018.

[91] M. Iqbal *et al.*, "Aqueous two-phase system (atps): An overview and advances in its applications," *Biological procedures online*, vol. 18, no. 1, pp. 1–18, 2016.

[92] C. H. T. Vu, H.-G. Lee, Y. K. Chang, H.-M. Oh, "Axenic cultures for microalgal biotechnology: Establishment, assessment, maintenance, and applications," *Biotechnology advances*, vol. 36, no. 2, pp. 380–396, 2018.

[93] P. Liu *et al.*, "Length-based separation of bacillus subtilis bacterial populations by viscoelastic microfluidics," *Microsystems & Nanoengineering*, vol. 8, no. 1, p. 7, 2022.

[94] G. M. Kim, Y.-K. Kim, "Drying techniques of microalgal biomass: A review," *Applied Chemistry for Engineering*, vol. 33, no. 2, pp. 145–150, 2022.

[95] Y. Wang *et al.*, "Serial separation of microalgae in a microfluidic chip under inertial and dielectrophoretic forces," *IEEE Sensors Journal*, vol. 20, no. 24, pp. 14 607–14 616, 2020.

[96] P. Sajeesh, A. K. Sen, "Particle separation and sorting in microfluidic devices: A review," *Microfluidics and nanofluidics*, vol. 17, pp. 1–52, 2014.

[97] M. Sivaramakrishnan, R. Kothandan, D. K. Govindarajan, Y. Meganathan, K. Kandaswamy, "Active microfluidic systems for cell sorting and separation," *Current Opinion in Biomedical Engineering*, vol. 13, pp. 60–68, 2020.

[98] S. Yan, J. Zhang, D. Yuan, W. Li, "Hybrid microfluidics combined with active and passive approaches for continuous cell separation," *Electrophoresis*, vol. 38, no. 2, pp. 238–249, 2017.

[99] Y. Zhang, T. Cole, J. Zheng, J. Guo, S.-Y. Tang, *et al.*, "Recent advances in non-optical microfluidic platforms for bioparticle detection," *Biosensors and Bioelectronics*, p. 114 944, 2022.

[100] Y. Wang, J. Wang, X. Wu, Z. Jiang, W. Wang, "Dielectrophoretic separation of microalgae cells in ballast water in a microfluidic chip," *Electrophoresis*, vol. 40, no. 6, pp. 969–978, 2019.

[101] M. Li, D. Li, Y. Song, D. Li, "Tunable particle/cell separation across aqueous two-phase system interface by electric pulse in microfluidics," *Journal of Colloid and Interface Science*, vol. 612, pp. 23–34, 2022.

[102] S.-I. Han, H. S. Kim, K.-H. Han, A. Han, "Digital quantification and selection of high-lipid-producing microalgae through a lateral dielectrophoresis-based microfluidic platform," *Lab on a Chip*, vol. 19, no. 24, pp. 4128–4138, 2019.

[103] M. Birkholz, D. E. Malti, S. Hartmann, P. Neubauer, "Separation of heterotrophic microalgae crypthecodinium cohnii by dielectrophoresis," *Frontiers in Bioengineering and Biotechnology*, vol. 10, p. 855 035, 2022.

[104] V. Varmazyari, H. Habibiyan, H. Ghafoorifard, M. Ebrahimi, S. Ghafouri-Fard, "A dielectrophoresis-based microfluidic system having double-sided optimized 3d electrodes for label-free cancer cell separation with preserving cell viability," *Scientific Reports*, vol. 12, no. 1, p. 12 100, 2022.

[105] M. Li, M. van Zee, K. Goda, D. Di Carlo, "Size-based sorting of hydrogel droplets using inertial microfluidics," *Lab on a Chip*, vol. 18, no. 17, pp. 2575–2582, 2018.

[106] A. Mihandoust, N. Maleki-Jirsaraei, S. Rouhani, S. Safi, M. Alizadeh, "Improvement of size-based particle separation throughput in slanted spiral microchannel by modifying outlet geometry," *Electrophoresis*, vol. 41, no. 5-6, pp. 353–359, 2020.

[107] A. Nikdoost, P. Rezai, "Dean flow velocity of viscoelastic fluids in curved microchannels," *AIP Advances*, vol. 10, no. 8, 2020.

[108] M.-L. Lee, D.-J. Yao, "The separation of microalgae using dean flow in a spiral microfluidic device," *Inventions*, vol. 3, no. 3, p. 40, 2018.

[109] R. Sharma, M. Kim, "Enhanced microalgae harvesting in a microfluidic centrifugal separator," *Biomass and Bioenergy*, vol. 159, p. 106 386, 2022.

[110] M. Li, H. E. Muñoz, K. Goda, D. Di Carlo, "Shape-based separation of microalga euglena gracilis using inertial microfluidics," *Scientific reports*, vol. 7, no. 1, p. 10 802, 2017.

[111] G.-Y. Kim, J. Son, J.-I. Han, J.-K. Park, "Inertial microfluidics-based separation of microalgae using a contraction–expansion array microchannel," *Micromachines*, vol. 12, no. 1, p. 97, 2021.

[112] G. Korensky *et al.*, "Single chlamydomonas reinhardtii cell separation from bacterial cells and auto-fluorescence tracking with a nanosieve device," *Electrophoresis*, vol. 42, no. 1-2, pp. 95–102, 2021.

[113] A. Hochstetter *et al.*, "Deterministic lateral displacement: Challenges and perspectives," *ACS nano*, vol. 14, no. 9, pp. 10 784–10 795, 2020.

[114] J. McGrath, M. Jimenez, H. Bridle, "Deterministic lateral displacement for particle separation: A review," *Lab on a Chip*, vol. 14, no. 21, pp. 4139–4158, 2014.

[115] Y. Wang, J. Wang, Y. Wu, J. Dong, "The automatic and high-throughput purification and enrichment of microalgae cells using deterministic lateral displacement arrays with different post shapes," *Journal of Chemical Technology & Biotechnology*, vol. 96, no. 8, pp. 2228–2237, 2021.

[116] H. Khashei, H. Latifi, M. J. Seresht, A. H. B. Ghasemi, "Microparticles manipulation and enhancement of their separation in pinched flow fractionation by insulator-based dielectrophoresis," *Electrophoresis*, vol. 37, no. 5-6, pp. 775–785, 2016.

[117] X. Lu, X. Xuan, "Inertia-enhanced pinched flow fractionation," *Analytical chemistry*, vol. 87, no. 8, pp. 4560–4565, 2015.

[118] M. Senaha, R. Mitamura, M. Yamada, M. Seki, "Two-dimensional cell sorting device employing pinched-flow fractionation and magnetophoresis," in *14th International Conference on Miniaturized Systems for Chermistry and Life Sciences*, 2010, pp. 1616–1618.

[119] S. Wang *et al.*, "Microalgae separation by inertia-enhanced pinched flow fractionation," *Electrophoresis*, vol. 42, no. 21-22, pp. 2223–2229, 2021.

[120] A. Fornell, H. Pohlit, Q. Shi, M. Tenje, "Acoustic focusing of beads and cells in hydrogel droplets," *Scientific Reports*, vol. 11, no. 1, p. 7479, 2021.

[121] M. Asghari *et al.*, "Oscillatory viscoelastic microfluidics for efficient focusing and separation of nanoscale species," *ACS nano*, vol. 14, no. 1, pp. 422–433, 2019.

[122] J. Zhou, I. Papautsky, "Viscoelastic microfluidics: Progress and challenges," *Microsystems & Nanoengineering*, vol. 6, no. 1, p. 113, 2020.

[123] D. Yuan *et al.*, "Sheathless separation of microalgae from bacteria using a simple straight channel based on viscoelastic microfluidics," *Lab on a Chip*, vol. 19, no. 17, pp. 2811–2821, 2019.

[124] H. S. Lim, J. Y. Kim, H. S. Kwak, S. J. Sim, "Integrated microfluidic platform for multiple processes from microalgal culture to lipid extraction," *Analytical chemistry*, vol. 86, no. 17, pp. 8585–8592, 2014.

[125] C. Nitsos, R. Filali, B. Taidi, J. Lemaire, "Current and novel approaches to downstream processing of microalgae: A review," *Biotechnology Advances*, vol. 45, p. 107 650, 2020.

[126] V. Timira, K. Meki, Z. Li, H. Lin, M. Xu, S. N. Pramod, "A comprehensive review on the application of novel disruption techniques for proteins release from microalgae," *Critical Reviews in Food Science and Nutrition*, vol. 62, no. 16, pp. 4309–4325, 2022.

[127] J. Yao, H. S. Kim, J. Y. Kim, Y.-E. Choi, J. Park, "Mechanical stress induced astaxanthin accumulation of h. pluvialis on a chip," *Lab on a Chip*, vol. 20, no. 3, pp. 647–654, 2020.

[128] X. Cheng, J. Riordon, B. Nguyen, M. D. Ooms, D. Sinton, "Hydrothermal disruption of algae cells for astaxanthin extraction," *Green Chemistry*, vol. 19, no. 1, pp. 106–111, 2017.

[129] B. Sert, B. İnan, D. Özçimen, "Effect of chemical pre-treatments on bioethanol production from chlorella minutissima," *Acta Chimica Slovenica*, vol. 65, no. 1, 2018.

[130] H. S. Kwak, J. Y. H. Kim, S. C. Na, N. L. Jeon, S. J. Sim, "Multiplex microfluidic system integrating sequential operations of microalgal lipid production," *Analyst*, vol. 141, no. 4, pp. 1218–1225, 2016.

[131] J. Wang *et al.*, "An integrated microfluidic chip for treatment and detection of microalgae cells," *Algal Research*, vol. 42, p. 101 593, 2019.

[132] Y. Song *et al.*, "Capacitive detection of living microalgae in a microfluidic chip," *Sensors and Actuators B: Chemical*, vol. 194, pp. 164–172, 2014.

[133] J. Wang, X. Meng, Y. Song, X. Pan, D. Li, "Detection of activity of single microalgae cells in a new microfluidic cell capturing chip," *Measurement Science and Technology*, vol. 27, no. 12, p. 125 701, 2016.

[134] N. Tripathi, A. Sapra, "Gram staining," 2020.

[135] R. Verhelst *et al.*, "Comparison between gram stain and culture for the characterization of vaginal microflora: Definition of a distinct grade that resembles grade i microflora and revised categorization of grade i microflora," *BMC microbiology*, vol. 5, pp. 1–11, 2005.

[136] S. Z. Tarhan, A. T. Koçer, D. Özçimen, I. Gökalp, "Utilization of hydrothermal process water for microalgae growth," *Eurasian Journal of Biological and Chemical Sciences*, vol. 3, no. 1, pp. 42–47, 2020.

[137] S. X. Z. Low *et al.*, "Viability of escherichia coli atcc 8739 in nutrient broth, luria-bertani broth and brain heart infusion over 11 weeks," *Electronic physician*, vol. 5, no. 1, p. 576, 2013.

[138] H. Fujikawa, S. Morozumi, "Modeling surface growth of escherichia coli on agar plates," *Applied and environmental microbiology*, vol. 71, no. 12, pp. 7920–7926, 2005.

[139] Q.-V. Do, D.-A. Van, V.-B. Nguyen, V.-S. Pham, "A numerical modeling study on inertial focusing of microparticle in spiral microchannel," *AIP Advances*, vol. 10, no. 7, 2020.

[140] S. Akgönül, A. Özbey, M. Karimzadehkhouei, D. Gozuacik, A. Koşar, "The effect of asymmetry on micromixing in curvilinear microchannels," *Microfluidics and Nanofluidics*, vol. 21, pp. 1–15, 2017.

[141] A. A. Aliero, F. Y. Turba, A. I. Bagudo, S. S. Manga, *et al.*, "Antibiotics resistant pattern of bacteria isolated from spoiled avocado fruit sold in sokoto metropolis," *Borneo Journal of Pharmacy*, vol. 5, no. 4, pp. 367–374, 2022.

[142] J. Han, S. Wang, L. Zhang, G. Yang, L. Zhao, K. Pan, "A method of batch-purifying microalgae with multiple antibiotics at extremely high concentrations," *Chinese Journal of Oceanology and Limnology*, vol. 34, no. 1, pp. 79–85, 2016.

[143] M. DuBois, K. A. Gilles, J. K. Hamilton, P. t. Rebers, F. Smith, "Colorimetric method for determination of sugars and related substances," *Analytical chemistry*, vol. 28, no. 3, pp. 350–356, 1956.

[144] O. Classics Lowry, N. Rosebrough, A. Farr, R. Randall, "Protein measurement with the folin phenol reagent," *J biol Chem*, vol. 193, no. 1, pp. 265–75, 1951.

[145] M. Macıas-Sánchez, C. Mantell, M. Rodrıguez, E. M. de La Ossa, L. Lubián, O. Montero, "Supercritical fluid extraction of carotenoids and chlorophyll a from nannochloropsis gaditana," *Journal of Food Engineering*, vol. 66, no. 2, pp. 245–251, 2005.

[146] N. Zou, A. Richmond, "Light-path length and population density in photoacclimation of nannochloropsis sp.(eustigmatophyceae)," *Journal of Applied Phycology*, vol. 12, pp. 349–354, 2000.

[147] J. A. Coronado-Reyes, J. A. Salazar-Torres, B. Juarez-Campos, J. C. Gonzalez-Hernandez, "Chlorella vulgaris, a microalgae important to be used in biotechnology: A review," *Food Science and Technology*, vol. 42, 2020.

[148] M. Vehapi, A. Yilmaz, D. Özçimen, "Antifungal activities of chlorella vulgaris and chlorella minutissima microalgae cultivated in bold basal medium, wastewater and tree extract water against aspergillus niger and fusarium oxysporum. rom," *Biotechnol. Lett*, vol. 1, pp. 1–8, 2018.

[149] H. N. Schulz, B. B. Jørgensen, "Big bacteria," *Annual Reviews in Microbiology*, vol. 55, no. 1, pp. 105–137, 2001.

[150] A. Kudryavtsev, C. Wylezich, M. Schlegel, J. Walochnik, R. Michel, "Ultrastructure, ssu rrna gene sequences and phylogenetic relationships of flamella schaeffer, 1926 (amoebozoa), with description of three new species," *Protist*, vol. 160, no. 1, pp. 21–40, 2009.

[151] V. Magalhães, V. Pinto, P. Sousa, L. Gonçalves, E. Fernández, G. Minas, "Spiral inertial microfluidics for separation and concentration of phytoplankton," *Algal Research*, vol. 76, p. 103 317, 2023.

[152] X. Luo, W. Zhang, H. Dong, A. K. Thakur, B. Yang, W. Zhao, "Numerical analysis of heat transfer enhancement of fluid past an oscillating circular cylinder in laminar flow regime," *Progress in Nuclear Energy*, vol. 139, p. 103 853, 2021.

[153] V. Omrani, M. Z. Targhi, F. Rahbarizadeh, R. Nosrati, "High-throughput isolation of cancer cells in spiral microchannel by changing the direction, magnitude and location of the maximum velocity," *Scientific Reports*, vol. 13, no. 1, p. 3213, 2023.

[154] N. Herrmann, P. Neubauer, M. Birkholz, "Spiral microfluidic devices for cell separation and sorting in bioprocesses," *Biomicrofluidics*, vol. 13, no. 6, 2019.

[155] Z. Wu, M. Zhao, Z. Liu, L. Shi, T. Li, T. Zhou, "Microalgae separation using spiral inertial microchannel," *Microfluidics and Nanofluidics*, vol. 27, no. 3, p. 23, 2023.

[156] A. A. S. Bhagat, S. S. Kuntaegowdanahalli, I. Papautsky, "Continuous particle separation in spiral microchannels using dean flows and differential migration," *Lab on a Chip*, vol. 8, no. 11, pp. 1906–1914, 2008.

[157] Y. Wang *et al.*, "A microfluidic prototype system towards microalgae cell separation, treatment and viability characterization," *Sensors*, vol. 19, no. 22, p. 4940, 2019.

[158] P. Bodénès, H.-Y. Wang, T.-H. Lee, H.-Y. Chen, C.-Y. Wang, "Microfluidic techniques for enhancing biofuel and biorefinery industry based on microalgae," *Biotechnology for biofuels*, vol. 12, pp. 1–25, 2019.

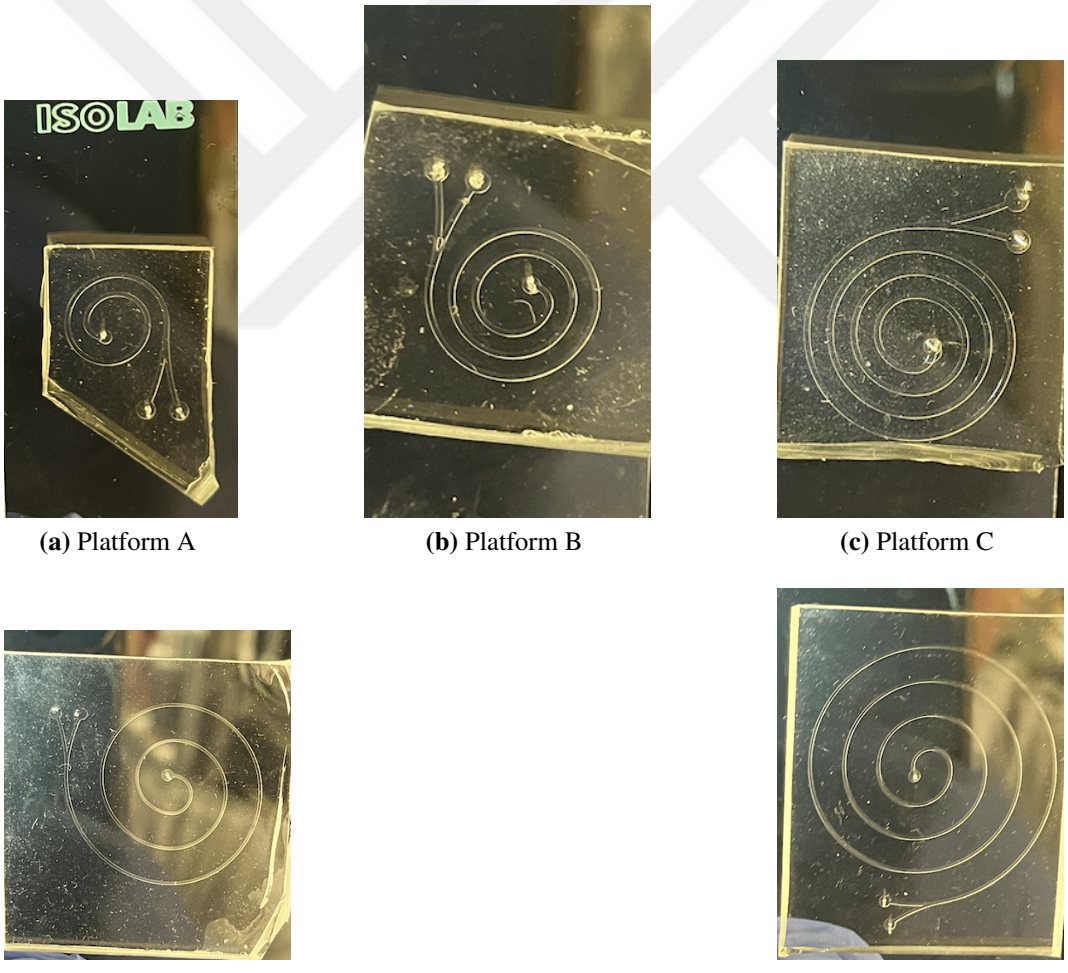
[159] L. Leng *et al.*, "Use of microalgae based technology for the removal of antibiotics from wastewater: A review," *Chemosphere*, vol. 238, p. 124 680, 2020.

[160] L. Sharma, G. Siedlewicz, K. Pazdro, "The toxic effects of antibiotics on freshwater and marine photosynthetic microorganisms: State of the art," *Plants*, vol. 10, no. 3, p. 591, 2021.

A APPENDIX CHAPTER HEADING

A.1 Microfabricated PDMS-based Microfluidic Platforms

Microfabricated PDMS-based microfluidic platforms with standard soft lithography method are shown in Figure A.1.



(a) Platform A **(b)** Platform B **(c)** Platform C

(d) Platform D **(e)** Platform E

Figure A.1 PDMS-based microfluidic platforms

PUBLICATIONS FROM THE THESIS

Papers

1. B. Karacaoğlu, B. İnan, D. B. Özçimen, “Microfluidic systems as a novel approach for microalgal bioprocess,” Biochemical Engineering Journal, vol. 197, p. 108 959, 2023.

Conference Papers

1. B. Karacaoğlu, İ. Bütün, R. Mercimek, B. İnan, D. Balkanlı, “Fabrication of a Microfluidic Platform for the Isolation of Polar Microalgae from Antarctica", AlgaEurope 2023, Prague-Czech Republic, 12-15 December 2023.

2. B. Karacaoğlu, D. Özçimen, “Microfluidic systems as a novel approach for microalgal bioprocess”, III. International Enzyme and Bioprocess Days (EBDays 2022), Tokat-Türkiye, 9-11 September 2022.

Projects

1. Design and Fabrication of a New Microfluidic Platform for the Separation of Microalgae from Samples with Mixed Microorganism Populations Obtained from Polar Regions, Republic of Türkiye Ministry of Industry and Technology, 1002 - Quick Support Program, July 2023.